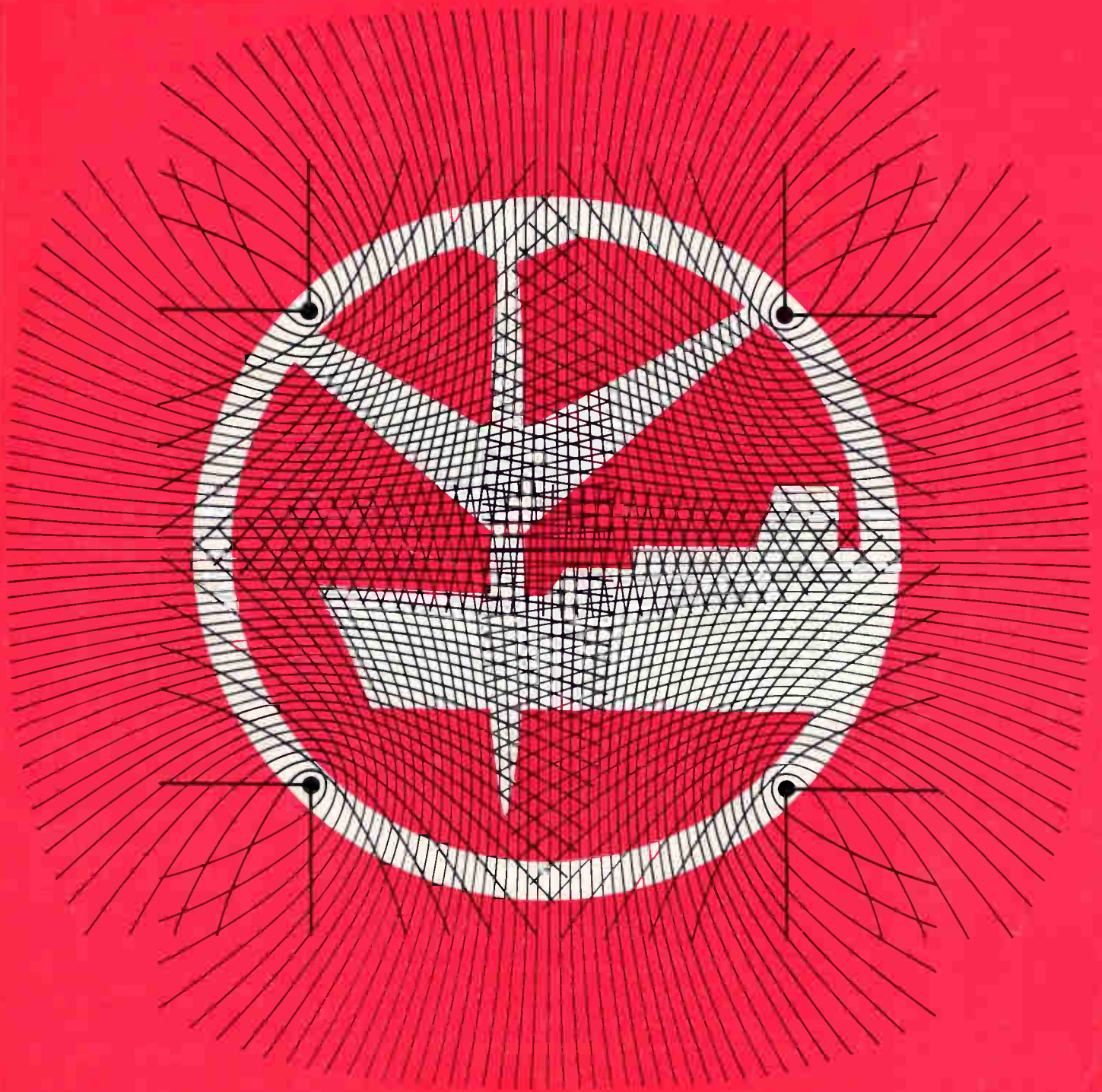


UNIVERSITY OF TORONTO



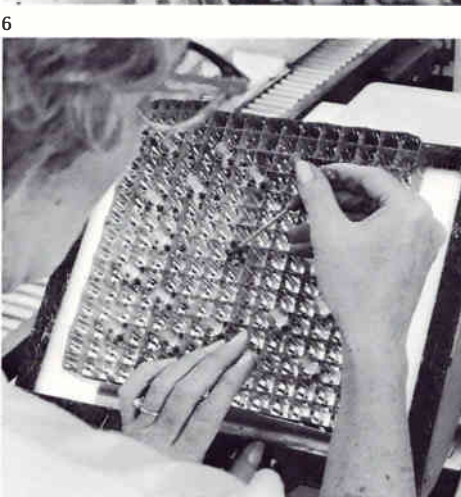
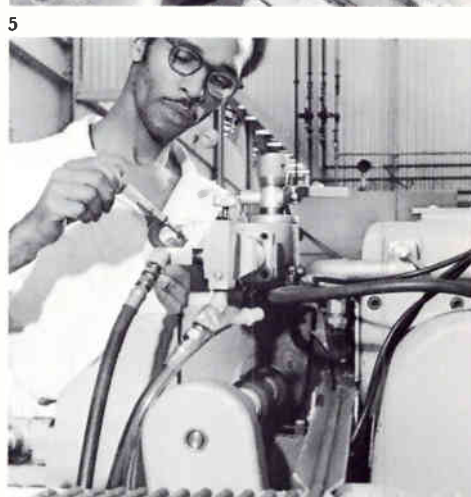
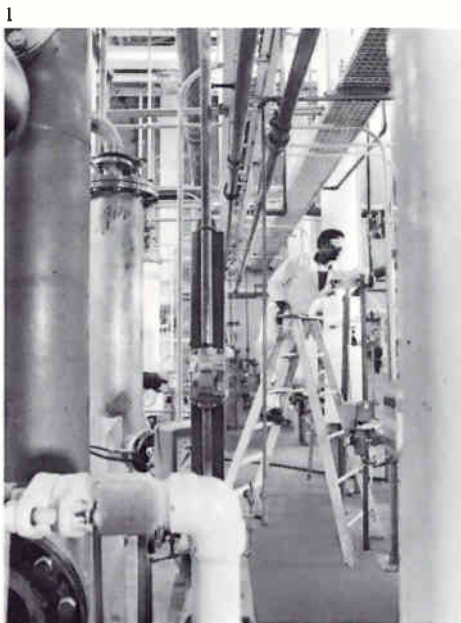
## Nuclear Reactor Fuel Assemblies Produced in New Plant

A nuclear fuel manufacturing plant has been opened at Columbia, South Carolina, as part of a major expansion program of the Westinghouse Power Systems Company to help meet the nation's rapidly growing demand for electric generating, transmission, and distribution equipment. The plant performs all operations necessary to manufacture nuclear fuel assemblies, which consist of arrays of precisely positioned fuel rods. The assemblies must be designed and built to give years of reliable service in demanding operating conditions.

Manufacturing begins with chemical conversion of uranium hexafluoride gas to ammonium diuranate by reactions with water and ammonium hydroxide (Fig. 1). The resulting slurry is centrifuged to separate the solid material (Fig. 2). The solid is then fed into a rotary calciner for conversion to uranium dioxide, which is pulverized and then granulated. The granules are pressed into fuel pellets of uniform density and size (Fig. 3), and the pellets are sintered in electric furnaces to consolidate their particles (Fig. 4).

Each pellet is then ground on a centerless grinder to the exact dimensions required (Fig. 5). The pellets are inserted into zircaloy tubes, and a plug is welded into each end of the tubes to form fuel rods.

Fuel-assembly support structures are fabricated to locate each fuel rod in a precise relationship to the others (Fig. 6). Finally, fuel rods and support structures are assembled to form completed fuel assemblies (Fig. 7). Water is sprayed onto the rods as they are inserted into the structure.



# Westinghouse ENGINEER

## July 1970, Volume 30, Number 4

5.00  
Engineering  
#3 @ 25

- 98 Transmitting Facilities for Omega  
W. S. Alberts
- 108 Control Computer Teaches Itself to Roll Metals  
A. W. Smith
- 114 Fast Valve Control Can Improve Turbine-Generator  
Response to Transient Disturbances  
O. J. Aanstad and H. E. Lokay
- 120 New Goals for EHV and Future UHV  
Power Circuit Breakers  
W. M. Leeds, R. E. Friedrich,  
T. E. Browne, Jr., and C. L. Wagner
- 125 Nonconsumable Electrode Makes Vacuum Arc Melting  
More Economical  
R. R. Akers
- 128 Technology in Progress  
Pittsburgh Stadium Gets Long-Life Maintenance-Free Floodlights  
Products for Industry

*Editor*  
M. M. Matthews

*Associate Editor*  
Oliver A. Nelson

*Assistant Editor*  
Barry W. Kinsey

*Design and Production*  
N. Robert Scott

*Editorial Advisors*  
S. W. Herwald  
T. P. Jones  
Dale McFeatters  
W. E. Shoupp

*Subscriptions:* United States and possessions,  
\$2.50 per year; all other countries,  
\$3.00 per year. Single copies, 50¢ each.

*Mailing address:* Westinghouse ENGINEER  
Westinghouse Building  
Gateway Center  
Pittsburgh, Pennsylvania 15222.

Copyright © 1970 by Westinghouse Electric  
Corporation.

Published bimonthly by the Westinghouse  
Electric Corporation, Pittsburgh, Pennsylvania.  
Printed in the United States by The Lakeside  
Press, Lancaster, Pennsylvania. Reproductions  
of the magazine by years are available on  
positive microfilm from University Microfilms,  
Inc., 300 North Zeeb Road, Ann Arbor,  
Michigan 48106.

*The following terms, which appear in this issue,  
are trademarks of the Westinghouse Electric  
Corporation and its subsidiaries:* Thermoguard;  
Durarc; Kovar; De-ion; Pulse-O-Matic;  
Adaptiflow.

*Front cover:* The Omega navigation system  
for ships and aircraft consists of a network of  
VLF transmitting stations, which provide an  
electronic lattice for determining position.  
Westinghouse participation in the development  
of the Omega system is described in the article  
that begins on the following page. The cover  
design is by artist Tom Ruddy.

## Transmitting Facilities for Omega

*The Navy Electronics Laboratory and the Naval Research Laboratory have cooperated in the development of the Omega worldwide navigation system, originally sponsored by the U.S. Navy Bureau of Ships and now by the Naval Electronic Systems Command. Development of the system was recommended by a radio-navigation steering committee composed of representatives of the Bureau of Ships, Office of Naval Research, the Naval Research Laboratory, the Navy Electronics Laboratory, the Chief of Naval Operations, the Bureau of Naval Weapons, and the Cruft Laboratory of Harvard University. Four stations of the eight-station Omega system are now in interim operation under*

*the Omega Project Office of the U.S. Navy. The Chesapeake Division, Naval Facilities Engineering Command, is the contracting agency for the designs of facilities for the operational system.*

*Westinghouse has participated in the project in many ways during the system development and interim testing phases, as well as in the present expansion to a fully operational system. The earlier work involved antenna site inspection and selection studies, site test measurements, design of interim facilities, consultation during construction and, in some cases, performance testing of finished test facilities. Westinghouse also supplied the AN/FRA-31 transmitters now in use at the three interim stations*

*operated by the United States.*

*More recent work on the operational Omega system facilities includes further site surveys and selections; cost effectiveness studies; preliminary and final designs of antennas, ground systems, and site buildings for U.S. and some foreign stations; and consultation, via the U.S. Navy, on other foreign stations being built by partner countries.*

*In virtually all of the work associated with Omega transmitting facilities, Westinghouse has teamed with the architect-engineering firm of Holmes & Narver, Inc., of Los Angeles to achieve integrated designs that carefully balance the electronic aspects with the architectural, civil, and structural disciplines.*



Omega is a worldwide navigational system that can be used at all times and under all weather conditions to determine ship or aircraft position quickly and accurately. Expected to be fully operational in 1973, the system will consist of eight very-low-frequency (VLF) transmitting stations, spaced around the world so that three to five stations will always be in range (Fig. 1). Very-low-frequency transmission provides the long-range highly stable transmission necessary to achieve the desired reliability with only eight stations worldwide. The system is capable of providing navigational accuracy of  $\pm$  one nautical mile in daytime and  $\pm$  two miles at night.

#### *Development of Omega*

The beginning of the Omega system came in 1947 when J. A. Pierce of Harvard University, a principal contributor to the Loran electromagnetic navigational system developed during World War II, recommended a redirection of effort in hyperbolic navigation from the time-difference principle used with Loran to a phase-difference technique. The initial result of this work was Radux, an experimental low-frequency system operated between the West Coast and Hawaii. With Radux, the Navy Electronics Laboratory demonstrated the stability of propagation for unmodulated carrier frequencies at 50 kHz and below. After further development on Radux, and then a two-frequency system (40 kHz and 10 kHz) called Radux-Omega, the preliminary work for the 10- to 14-kHz Omega system began in 1957.

The first experimental Omega system began operation in the early 1960's. It permitted a thorough evaluation of VLF phase-difference measurement for a navigational system. Stations were located in the Canal Zone, Hawaii, New York State,

and Great Britain. Those sites were chosen for the availability of existing antennas and buildings rather than for the most favorable geometry. However, the excellent results obtained with the experimental system led to the worldwide Omega system now being installed.

The Omega system *now in operation* consists of four transmitter stations in interim operation (Table I). These four stations provide coverage to about one-fourth of the world. In the full-power operational system, three of the present stations will be upgraded and one will be replaced; four new stations will be added in appropriate areas (Fig. 1).

#### *Omega System Operation*

Position is determined by measuring phase difference between phase-stable, accurately time-synchronized carrier signals from three or more VLF transmitters. Lines drawn through the points where the signals from any pair of stations are in phase form a grid of hyperbolic curves (Fig. 2). These zero-phase-difference lines bound lanes approximately 8 miles wide (one-half wavelength at 10.2 kHz) along the baseline between stations. Since phase-difference measurements vary between zero and 360 degrees in every lane, the measurements are ambiguous unless the navigator knows which lane he is in, or has knowledge of his position to within four miles through some other navigational reference to establish lane number.

The measurement ambiguity is handled by designing the Omega receiver to "count" lanes in one fashion or another. In the simplest form of shipboard receiver, phase difference is continuously recorded on a strip-chart recorder. The navigator manually numbers lanes as they are crossed on the chart. (See *Determining Position with Omega*. Note that charts are calibrated in *centilanes*, or hundredths of a lane, rather than phase-difference degrees.) In more sophisticated Omega receivers, lane counting is done automatically by receiver circuitry.

By determining the lane number and the position of the receiver within the lane, a line of position (LOP) can be drawn on an Omega navigational chart.

The process is repeated for another pair of Omega stations, another line of position established, and the intersection of the LOPs provides the navigational fix. In computerized versions of the Omega receiver, position is computed automatically and position coordinates are displayed directly.

The accuracy of the fix is limited by variations in signal propagation with the changing height of the ionosphere from day to night, the nature of the earth's surface over which the signals travel, and other conditions. With existing knowledge of these effects, Omega skywave correction factors provide accuracies of  $\pm$  one nautical mile by day and two by night.

#### *Omega Signal Format*

When the worldwide Omega system is completed, each station will transmit three basic frequencies for navigational purposes: 10.2, 11.33, and 13.6 kHz. The timing sequence and differences in pulse length permit the station to be identified (Fig. 3). In addition to the three basic navigational frequencies, each station will also be assigned two unique frequencies that can be transmitted during the remainder of the 10-second period when it is not transmitting the basic navigational pulses. The system may use these unique signal frequencies for such additional navigational information as station identification, frequency standard, time standard and internal communication.

Each of the three basic frequencies establishes a unique family of lanes between each pair of stations within range of the receiver. Thus, the signal format provides in effect three independent single-frequency Omega systems. A manually switchable shipboard receiver can track lines of position on each of the basic frequencies, or successively on two or three of these frequencies.

The three basic frequencies have been chosen so that their difference frequencies can be used to generate wider lanes to resolve lane ambiguity. For example, the difference frequency of the 10.2- and 13.6-kHz signals is 3.4 kHz, which can be used to generate a family of hyperbolic lanes 24 miles wide (one-third of 10.2 kHz,

W. S. Alberts is Consulting Engineer at DECO Communications Department, Westinghouse Defense and Space Center, Leesburg, Virginia.

*Left*—A scale model of a Trinidad mountain valley spanned by a multiwire radio antenna is used by Westinghouse engineers to test the antenna characteristics to help the Navy select sites and design transmitting facilities.



- Final Site, Interim Operation
- ▨ Temporary Site, Interim Operation
- Station to be Constructed
- Awaiting Site Selection

three times the lane width). When utilizing the 3.4-kHz difference frequency, the navigator need only know his position to within  $\pm 12$  miles to establish lane count. A line of position developed within this 24-mile lane can be used to identify the narrower 8-mile 10.2-kHz lane. Similarly, the difference frequency between 10.2 and 11.33 kHz can be used to resolve ambiguities within a 72-mile lane.

### Transmitting Antennas

A conventional transmitting antenna configuration used for standard AM broadcast stations in the medium-frequency range is the single vertical radiator, which usually has a height of about one-quarter to one-half wavelength at the station's operating frequency. However, a similar antenna at the 10.2-kHz Omega frequency in the VLF portion of the frequency spectrum would be 5 to 10 miles high. Thus, VLF antennas must be limited to a small portion of this desired height. However, such height restrictions impose a severe burden on the overall efficiency of the

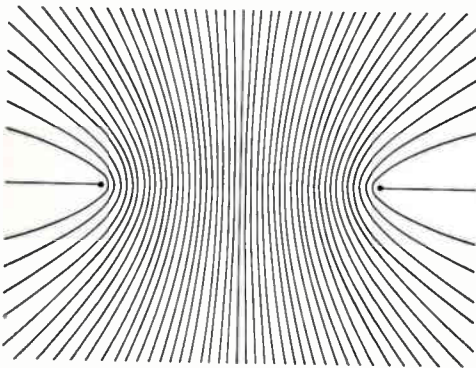
antenna and its associated ground system and tuning network. To achieve acceptable system efficiency at these low frequencies, the conventional radiator configuration is normally modified by adding an array of "top loading" conducting cables to form a large capacitor relative to ground. This alternate configuration allows the antenna to carry higher currents and thus radiate more energy than a simple vertical antenna of the same height and operated at the same voltage.

Two forms of top-loaded antennas are used in the Omega system. One is the umbrella-shaped array, which will be used for at least three of the Omega stations (Table I). A typical antenna is the North Dakota installation (Fig. 4) with a central tower 1200 feet in height. Its top-loading radials are anchored 2400 feet from the tower base and are active for 60 percent of their total length. The ground plane consists of a radial network of buried copper wires, 3000 feet in diameter.

The other basic antenna configuration used for the Omega stations is the "valley-span" arrangement (Fig. 5). This configuration consists of cables strung between two mountain ridges to provide the top-load area. The ground plane can be a network of conductors covering the valley floor, or, if the antenna spans a fjord (as for the Bratland, Norway, site), salt water provides the major portion of the ground plane.

### Tuning Networks

The impedance of an Omega transmitting antenna is typical of electrically short antennas, the type necessarily used in VLF radiating systems—a very low resistance component and a highly capacitive reactance component. Impedance matching is accomplished by means of a tuning network with large series inductance. In this manner, the antenna capacitive reactance is cancelled, leaving only the resistive component composed of the radiation resistance and the loss resistances in the radiation system. The

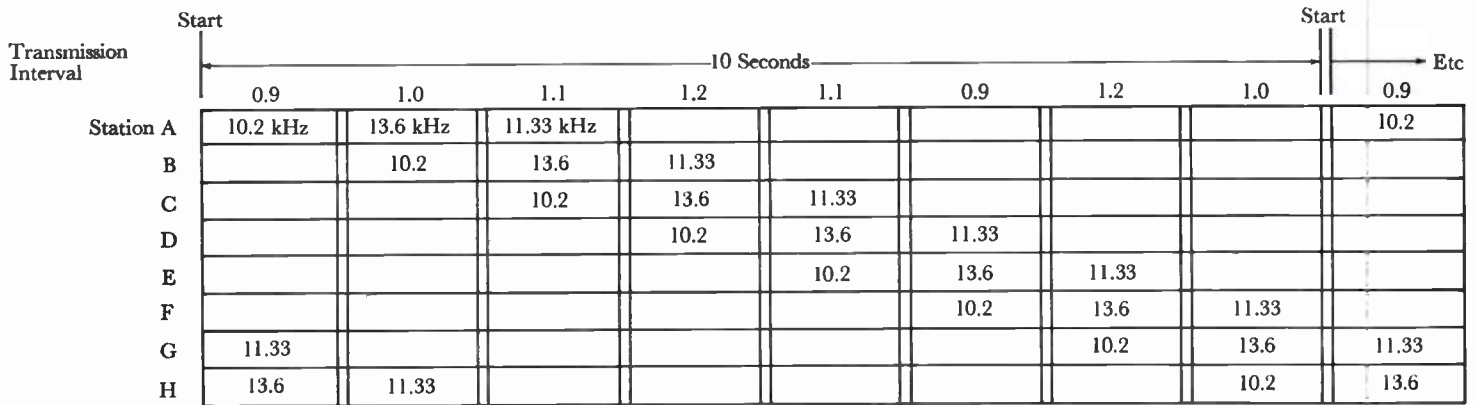


1—(Left) Omega system sites are situated around the world so that a ship can always receive signals from at least three transmitters. Present status of the sites is given in Table I.

2—(Above) Phase cancellation between two Omega transmitters occurs every half wavelength between stations, creating "lanes" of 8-mile width (along the baseline at 10.2 kHz). Receiver counts integral lanes and determines a line of position within the lane by phase-difference measurement.

Table I. Summary of Omega Navigation System

Sites	
North Dakota (La Moure)	Will replace New York (Forestport) low-power operation
Hawaii (Haiku)	Currently medium-power operation
Trinidad	Currently medium-power operation
Norway (Bratland)	Currently medium-power operation
Japan	New site
La Reunion (Indian Ocean)	New site
Argentina	New site
Australia—New Zealand area	Site to be selected
Operational System Characteristics	
Frequency	10 to 14 kHz
Radiated power	10 kW minimum
Transmitter power	150 kW
Coverage capability	Global
Accuracy	$\pm 1$ mile, day; $\pm 2$ miles, night
Antennas	
Top-loaded vertical (umbrella)	North Dakota, Argentina, Japan
Valley or fjord spans	Hawaii, Trinidad, Norway, La Reunion
Undetermined	Australia—New Zealand



**Planned Omega Station Assignments:**

- A Norway (Bratland)
- B Trinidad
- C Hawaii (Haiku)
- D New York (Forestport), Eventually North Dakota
- E La Reunion
- F Argentina
- G Australia—New Zealand
- H Japan

**Determining Position with Omega**

A navigational fix is obtained by plotting the intersection of two or more lines of position (LOPs). The three requisites for plotting Omega LOPs are a phase-difference-measuring VLF receiver, hyperbolic navigational tables and/or charts, and applicable skywave correction tables. (Hyperbolic charts and tables are published by the Navy's Oceanographic Office.)

The Omega lane and centilane count are obtained from the receiver. For example, if the receiver uses a strip-chart recorder, the integral lane count can be maintained by direct manual entry on the strip chart (a). The centilane count is added to the lane

count to obtain the observed receiver reading ( $T_*$ ). This reading must then be corrected by algebraically applying the appropriate skywave correction ( $SWC$ ) for the time, date, and approximate position (b) to obtain the corrected receiver reading ( $T_G$ ). The LOP for this corrected receiver reading is plotted by interpolation on the navigational chart (c).

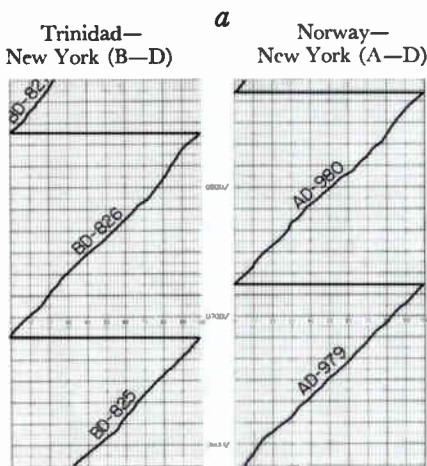
For example, assume a ship in the North Atlantic on January 10 is traveling a course (C) of 320 degrees at a speed (S) of 20 knots. The ship's navigator is obtaining the 0700Z fix (Greenwich Mean Time). The ship's 0700Z DR (dead reckoning) position

is 15° 16.0' N, 40° 23.5' W.

From the receiver strip charts (a) for two Omega station pairs—Trinidad—New York (B—D) and Norway—New York (A—D)—and the corresponding skywave correction tables (b), he obtains two corrected receiver readings:

	B—D		A—D
$T_s$	826.10	$T_s$	979.83
$SWC$	+0.18	$SWC$	-0.35
$T_G$	826.28	$T_G$	979.48

The corrected readings are plotted by interpolation on the chart (c), providing two intersecting LOPs for the 0700Z fix.

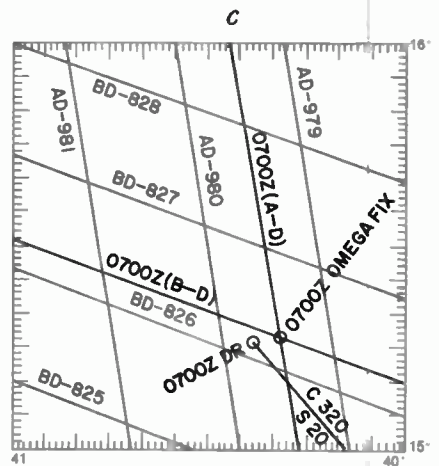


**b**

		LOCATION: 16.0° N 40.0° W LOP: B-D TRINIDAD-NEW YORK									
GMT	01	02	03	04	05	06	07	...	24		
DATE	01	18	18	18	18	18	18	...	18		
	1-15 Jan	18	18	18	18	18	18	...	18		
	16-31 Jan	18	18	18	18	18	18	...	18		
	1-14 Feb	18	18	18	18	18	18	...	18		
	...										
	16-31 Dec	18	18	18	18	18	18	...	18		

		LOCATION: 16.0° N 40.0° W LOP: A-D NORWAY-NEW YORK									
GMT	01	02	03	04	05	06	07	...	24		
DATE	01	-35	-35	-35	-35	-35	-35	...	-35		
	1-15 Jan	-35	-35	-35	-35	-35	-35	...	-35		
	16-31 Jan	-35	-35	-35	-35	-35	-35	...	-35		
	1-14 Feb	-35	-35	-35	-35	-35	-35	...	-35		
	...										
	16-31 Dec	-35	-35	-35	-35	-35	-35	...	-35		

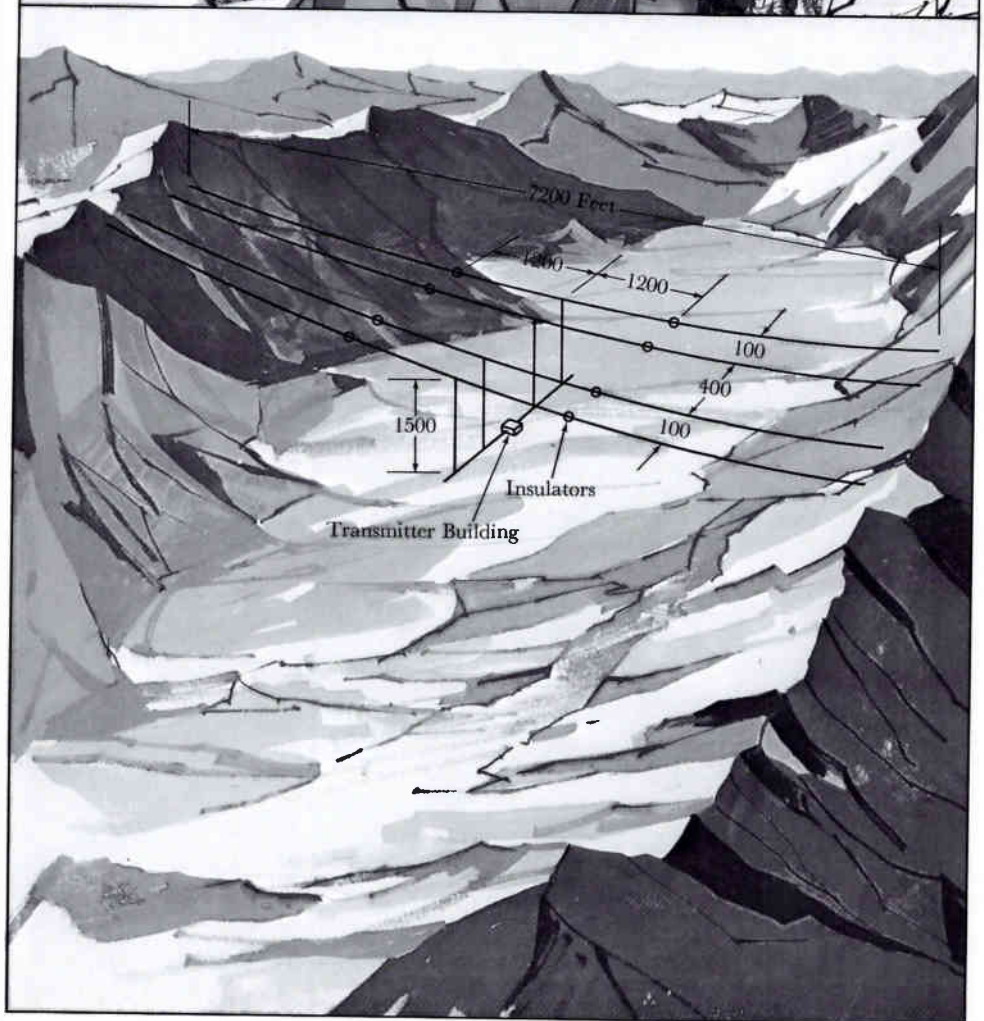
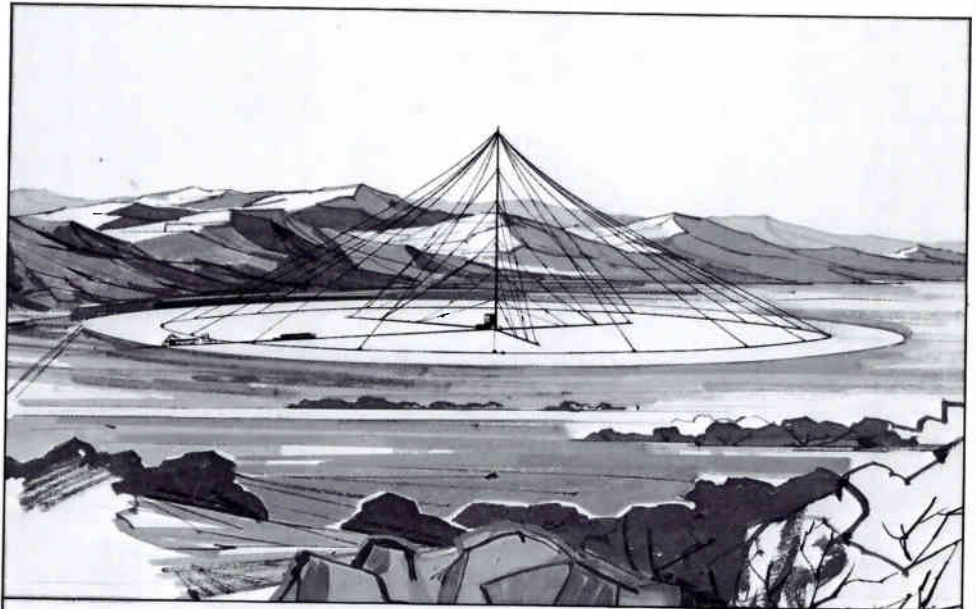


**Note:** The format of tables now available from the Oceanographic Office presents the skywave correction in a single-station (range) mode so that the skywave correction for a station pair must be determined by algebraically combining the corrections from each station of the pair.

resistive component is properly matched to the final amplifier by an RF transformer that is a part of the Omega transmitter.

The total system inductance requirements for each of the eight Omega sites varies with the static capacitance of the antenna under consideration. The predicted antenna characteristics and the estimates of the tuning requirements for the eight Omega sites are shown in Table II. The range of total inductance needed to accommodate the eight sites varies from approximately 4.7 to 9.2 millihenries.

The *variable* portion of the total inductance required at each site is determined by estimating the change in static capacitance under maximum environmental conditions such as wind or ice loading. To determine representative changes in static capacitance of valley-span antennas under wind load, a thorough analysis was made of the Haiku and Trinidad antennas. Structural investigations were made by Westinghouse's Omega architect-engineer teammate, Holmes & Narver, Inc., to determine the change in span coordinates for these two antennas under a wind load of 70 mi/h at the antenna base. The vertical deflection of the spans under wind load tends to decrease the antenna capacitance by increasing span height. The capacitance change was found to be about 4.0 and 3.5 percent for the Haiku and Trinidad antennas, respectively. Assuming these cases to be typical, the maximum decrease in static capacitance of the valley-span type antenna under wind load is approximately 4.0 percent.



3—(Above left) The Omega signal format is shown as it will be when all eight stations are operational. Undesignated intervals may be assigned either of two unique frequencies for each station for identification and other navigational information.

4—(Above right) Umbrella-shaped antenna will be used for the La Moure, North Dakota, site and others.

5—(Right) Haiku, Hawaii, valley-span antenna site shows the dimensions of the interim antenna. This antenna will be upgraded to a total of six spans for the operational station.

A factor tending to compensate for the decrease in capacitance of the antenna is a slight increase in inductance of the downlead under wind load as a result of the increase in the angle between the horizontal and vertical portions of the downlead at the hinge point, which partially reduces the above percentages.

The tuning networks of the Omega transmitting facilities differ in several respects from those employed in typical VLF or LF communications transmitting facilities. These differences result primarily from the signal format upon which the navigation system is based (Fig. 3). This format requires the transmission of a number of discrete frequencies, each being transmitted for approximately one second, followed by an off-air period of 0.2 second to permit time to adjust the tuning network to the next frequency. Since the value of inductance required to resonate the antenna differs for each frequency transmitted, means must be provided to switch the inductance within the available off-air time periods and at the appropriate intervals.

Although the antenna and ground systems vary at each of the eight facilities, the basic requirements of the tuning network allow an appreciable degree of commonality, which helps minimize cost through quantity procurement and also simplifies operation and maintenance.

The basic tuning network configuration follows the general guidelines established by the Naval Electronics Laboratory Center and is similar in concept to that presently in use with the interim transmitter and antenna system at the Trinidad Omega facility.

The primary function of the tuning network is to match the high-power RF energy from the transmitter to the antenna. An associated function of the tuning network is to perform certain control and monitoring tasks.

The matching function of the tuning network is accomplished with a large tapped inductor (helix), six variable inductors (variometers), six high-voltage vacuum switches (antenna relays), and associated RF buswork (Figs. 6 and 7). An antenna grounding switch, personnel interlock safety switches, disconnects, and two antenna grounding relays are required for auxiliary functions.

The control and monitoring functions include the mechanical group drive system for the variometers, remote controls and indicators, drive units for the antenna relays, a remote control system for the antenna grounding switch, etc.

*Helix Design*—The helix inductance for a given site will be that total tuning network inductive reactance necessary to cancel antenna base reactance less the variometer inductance at its reference or

“quiescent” setting and stray inductance in the interconnecting RF buswork and switching circuits.

A solenoid form wound of Litz wire was the most economical method found for obtaining the high performance characteristics required for the Omega radiation system. The basic helix configuration is a coil 14 feet in diameter with a winding pitch of  $4\frac{1}{2}$  inches. Since helix diameter will be the same for all sites, the number of turns required will vary from about 40 to 80. The height of the vertical support members will be varied in modular increments to accommodate different numbers of turns.

A constant conductor size (2.6-inch diameter) will be used for all helixes. The conductor size is dictated by the current required to radiate 10 kW at the antenna site estimated to have the lowest radiation resistance. That site is Trinidad, with an estimated radiation resistance of 0.022 ohm. In order to radiate 10 kW at 10.2 kHz with this value of resistance, an antenna base current of approximately 700 amperes is required. This dictates a Litz conductor cross-section of approxi-

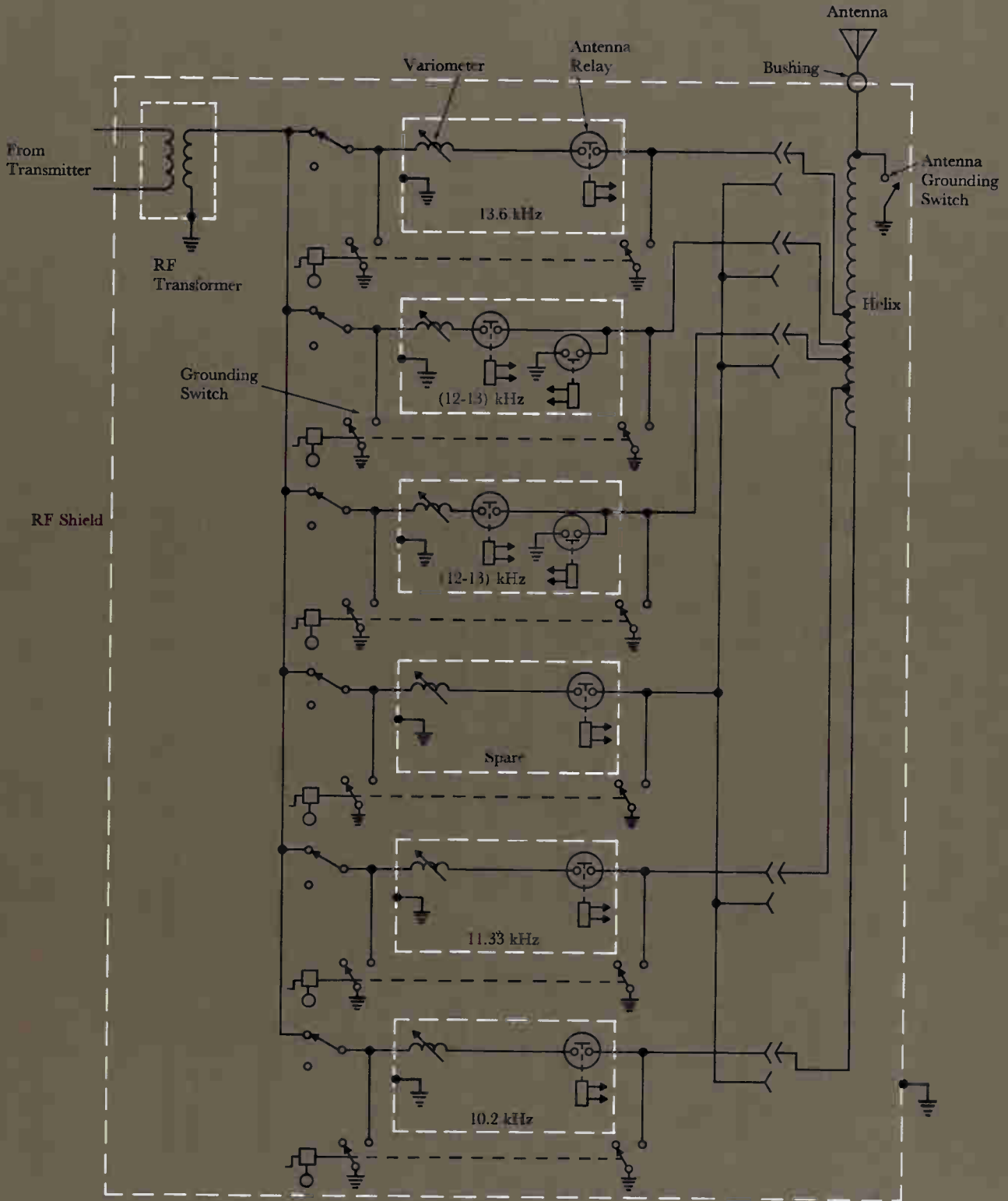
6—The antenna tuning network consists of the main helix, six variometers, and six antenna relays for switching the network to conform with the Omega signal format.

Table II. Antenna Characteristics<sup>1</sup> and Circuit Inductance Requirements of Proposed Omega Sites

Site	Effective Height (ft)	Static Capacitance ( $\mu$ f)	Resonant Frequency (kHz)	Radiation Resistance (ohms)	Base Current <sup>2</sup> (A)	Approx Circuit Inductance (mH)
North Dakota (La Moure)	646	0.0267	53.2	0.0709	375	8.783
Hawaii (Haiku)	492	0.0420	39.0	0.0411	493	5.400
Trinidad	361	0.0480	39.0	0.0221	672	4.725
Norway (Bratland)	708	0.0318	30.4	0.0853	342	6.792
Japan	699	0.0260	56.0	0.0829	347	9.159
La Reunion (Indian Ocean)	590	0.0310	34.0	0.0592	411	7.147
Argentina	646	0.0267	53.2	0.0709	375	8.783
Australia—New Zealand	525	0.0310	35.0	0.0468	462	7.187

<sup>1</sup>Values given for antennas presently being designed or contemplated except for Australia—New Zealand, where values are for one of several sites investigated.

<sup>2</sup>For 10-kW radiated power at 10.2 kHz.



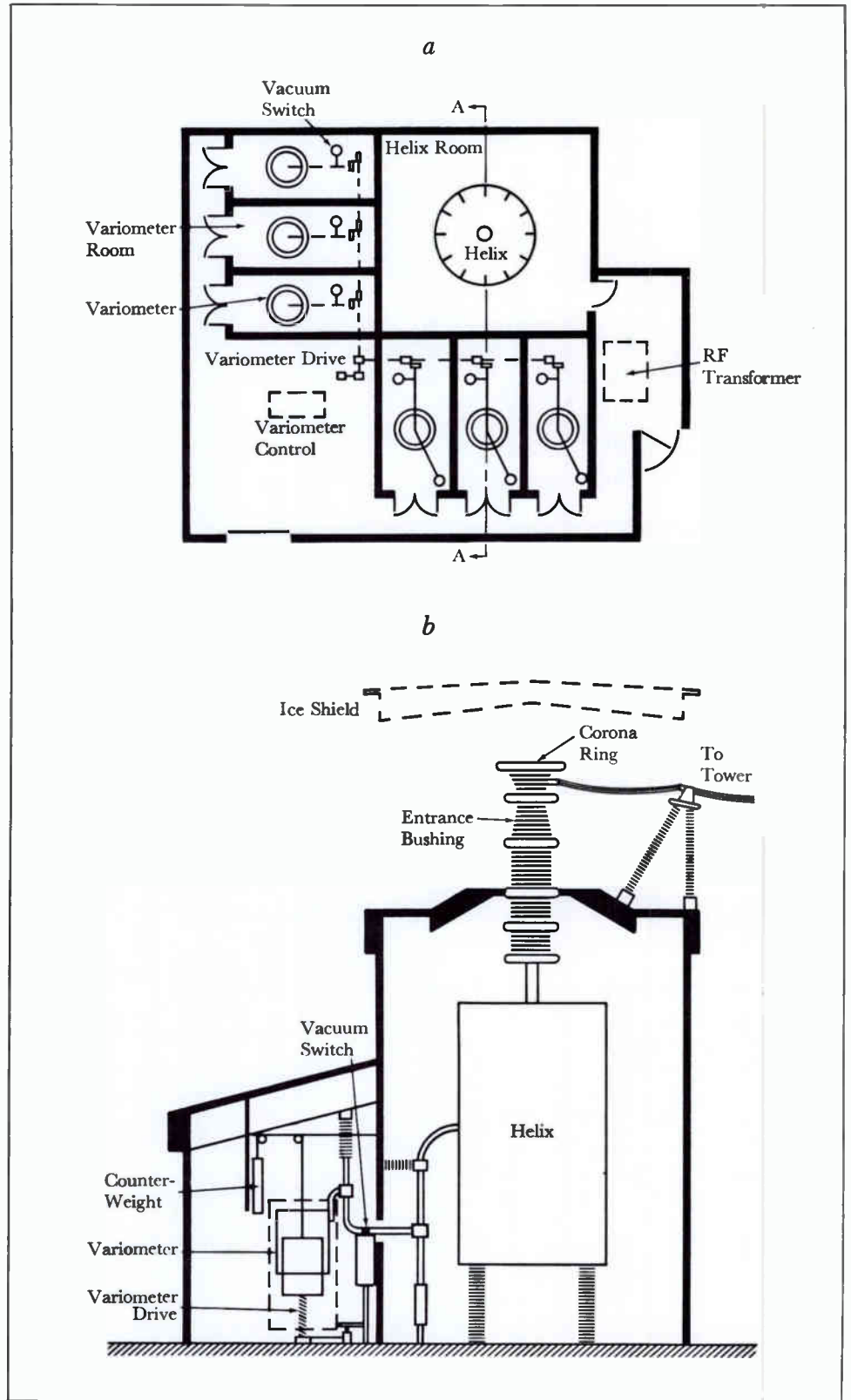
mately 700,000 circular mils, which has a nominal diameter of 2.6 inches.

The voltage gradient on the surface of the helix conductors and associated buswork leading to the RF feed-through bushing must be controlled to avoid corona or possible flashover. The voltage at the upper portion of the helix is maximum at the lowest operating frequency (10.2 kHz). This voltage is equal to the antenna base current times the antenna base reactance. The highest voltage is not expected to exceed approximately 220 kV. The coil tends to be self-grading; however, the final upper turns must be carefully considered to avoid developing gradients which exceed approximately one kV/mm.

The highest voltage present on the helix conductors also requires that the support material used for the coil form have suitable loss and dielectric strength characteristics. The support frame material must be suitable structurally and the design must firmly support the conductors to prevent movement when the RF power is applied.

The helix will be tapped at a number of points to accommodate the several Omega frequencies. There will be a tap associated with each frequency in the station signal format. The tap location for a given frequency must consider the total inductance in the tuning network, i.e., the sum of the tapped portion of the helix, the variometer at its quiescent setting, and the stray inductance in the RF buswork and switches. To operate the variometer at its most effective point, the helix tap should be within a tolerance of approximately  $\pm 50$  microhenries, which corresponds to approximately  $\pm$  one-half turn for the average helix.

7—Section and plan views of the helix building for the La Moure, North Dakota, Omega navigation station. The building is located adjacent to the tower antenna. It houses the helix coil, the six tuning variometers and their associated drive mechanisms, the six antenna relays, and the RF matching transformer. A bushing in the center of the helix-room ceiling feeds the VLF signal through the roof to the download pull-off structure.



For the three basic frequencies common to all sites, the relative tap positions have been roughly estimated for a typical umbrella antenna configuration. The 10.2-kHz tap will be at the bottom of the helix, the 11.33-kHz tap will be approximately 20 percent above the bottom, and the 13.6-kHz tap will be approximately 45 percent above the bottom. The two taps for the two unique frequencies will be located somewhere between the other tap locations, depending upon the frequencies assigned to the station.

**Variometer Design**—The tuning network must also include provisions for continuously varying circuit inductance to accommodate tolerances in the major elements of the system and to compensate for small variations in antenna impedance resulting from distortion of the antenna configuration due to wind load or other environmental factors.

Six variometers provide continuously variable inductance for the antenna tuning network. Each variometer assembly consists of two vertical concentric coils. The outer fixed coil is approximately five feet in diameter and six feet high. It has 35 turns of 1.6-inch diameter Litz cable, connected in series with the antenna circuit when the variometer is active. The inner movable coil is also approximately six feet high and contains the same number of turns of the same size conductor. Its ends are connected to each other to short circuit the coil. The inductance is varied by moving the shorted inner coil vertically within the fixed outer coil by a screw jack. The weight of the inner coil is supported by a counterweight and cable system. Since the variometers have a lower duty cycle than the helix, current heating is lower and the coils can be wound of smaller conductor.

Since the  $Q$  (reactance versus resistance) value of the helix is appreciably higher than that of the variometer, the variometer is designed with the minimum inductance consistent with the required inductance variation. The variometer inductance range was determined at 10.2 kHz because the antenna capacitive reactance decreases directly with increases in frequency and the inductive reactance of the variometer increases

with frequency. Furthermore, since all variometers are identical, the maximum variometer inductance required to tune out the variance in antenna reactance was computed for the valley-span antenna with the lowest static capacitance. The variometer movement requirement varies approximately inversely with the square of frequency. The total variable inductance requirement established for each variometer is approximately 600 microhenries. The above configuration meeting this requirement has a minimum inductance of about 500 microhenries.

**Antenna Relays**—Major increments of inductance in the antenna circuit are obtained rapidly by means of appropriate taps on the helix with circuit connections to the taps made through high-voltage vacuum switches, called antenna relays. The antenna relays switch the tuning network sequentially to each of the five required frequencies and ground the helix if any frequency transmission is deleted from the normal sequence.

The voltage and current-carrying requirements of an antenna relay and its operational reliability requirements are severe. A relay that has performed well at the stations now in operation consists of a composite switch assembly of three vacuum-switch cells, electrically connected in series. The switch cells are actuated in unison through tandem dielectric shafts connected to a single solenoid.

#### **Present Status of Omega**

Omega will be the first navigation system to provide continuous worldwide all-weather coverage. The one- to two-mile accuracy will meet the general navigational needs of hundreds of Navy ships and aircraft. The system will also be useful for civilian navigation, both U.S. and foreign.

The four existing stations are now in regular operation, three operated by the U.S. and the Bratland station operated by Norway. Foreign countries have been asked to build and operate the four additional new stations required.

The three interim Omega stations operated by the U.S. use the AN/FRA-31 transmitter, which was originally design-

ed as a low-frequency transmitter for the Radux system. These transmitters provided a clean 100-kW output when operated at their design frequency, but produced square waves in the range of 9 to 14 kHz. However, the high  $Q$  of the antenna and tuning systems made this unimportant. Thus, the interim equipment made optimum use of an existing design, with only those modifications required to handle the new requirements of the Omega application.

Of the four existing stations, the low-power station at Forestport, New York, on loan from the Air Force, will be replaced by a new station in North Dakota. The station in Norway will be provided with permanent buildings and an improved antenna. The stations in Trinidad and Hawaii will both have antenna improvements to permit a radiated power of 10 kW and will have buildings altered to permit installation of new full-power electronic equipment.

The existing stations are now radiating power from about 200 watts to about 3 kW. The Navy is presently replacing these interim transmitters with new equipment that, in conjunction with the improvements in the antenna and ground systems, will bring radiated power to a minimum of 10 kW.

#### **REFERENCES:**

- <sup>1</sup>J. W. Brogden, A. W. Coven, and M. F. Williams, "The Omega Navigation System," *Frequency*, March-April 1963.
- <sup>2</sup>E. R. Swanson and M. L. Tibbals, "The Omega Navigation System," *NAVIGATION: Journal of the Institute of Navigation*, Vol. 12, No. 1, Spring 1965.
- <sup>3</sup>John I. Dick-Peddie, "Sites for Omega Navigation System," *THE MILITARY ENGINEER*, May-June 1968.
- <sup>4</sup>"A Fix for the Errant Mariner," *Business Week*, January 11, 1969.

# Control Computer Teaches Itself to Roll Metals

Andrew W. Smith

*Most computers that control rolling mills require much off-line data analysis and adjustment of mathematical models to optimize production performance, especially when starting up and when product characteristics change. A new adaptive control system, however, greatly speeds the optimizing process by adjusting the model predictions on line as data is collected during the rolling of each piece.*

One of the major frustrations when installing a computer control system is the length of time required to get the system to its optimum level of performance. Because actual shop operation always varies somewhat from the behavior predicted for it, thousands of minute control adjustments and changes have to be made. In a steel rolling mill, the problem is further complicated by the number of grades (determining hardness) and sizes of steel to be rolled, each requiring slightly different handling. Some mills roll a seemingly infinite variety of grade and size combinations, with some of the combinations appearing very infrequently.

In the past, the required changes in control programming had to be made by checking operation and correcting or modifying control programs to obtain satisfactory performance on each grade as it appeared. The problem was solved last year, at least for steel rolling mills, by a new adaptive control technique developed by Computer and Instrumentation Division engineers. The method allows the computer to teach itself how steel must be rolled in that mill, and to correct its own instructions within a very short time after a new grade or size is encountered.

The method was first developed for use with a hot strip mill at the Gadsden Works of Republic Steel Corporation. That mill handles many products on an infrequent basis, some as seldom as once in six months, but the success of adaptive control was clear after only a part of the products had been checked out. The sys-

tem has since been used on a new strip mill at Youngstown Sheet and Tube Company, East Chicago, with the same success.

## **Typical Hot Strip Mill**

To understand the new system, it is first necessary to understand something of how a hot strip mill works and the types of control previously available. In a typical mill, steel slabs are heated to rolling temperature in one or more furnaces, then moved to a roughing mill where they are reduced (in three to nine passes) from a thickness of 5 to 10 inches to a bar approximately 1 to 1½ inches thick. (Most hot strip mills have a number of roughing-mill stands in succession, but use of a one-stand reversing roughing mill is assumed in this article to better illustrate the learning procedure.)

The steel then moves to a finishing mill, which consists of several stands in succession. It completes the reduction of thickness to a finished strip 0.050 to 0.500 inch thick, 20 to 80 inches wide. The speed of the individual stands in the finishing mill must be precisely controlled, with successive stands running at higher speeds because strip length increases as thickness is reduced. Looper rolls between the stands control tension on the strip, and a coiler receives the finished product for storage.

Most of the newer hot strip mills have on-line computer control systems. Input data to the computer include slab dimensions, grade identification, and desired strip width and thickness.

Computer control systems usually have the ability to control the adjustments that regulate thickness and width of the product being rolled. The computer determines the number of passes and the thickness and width to be delivered from each pass in the rougher, the thickness of the product to be delivered from each of the finishing stands, and the speed with which the product is moved through the stands.

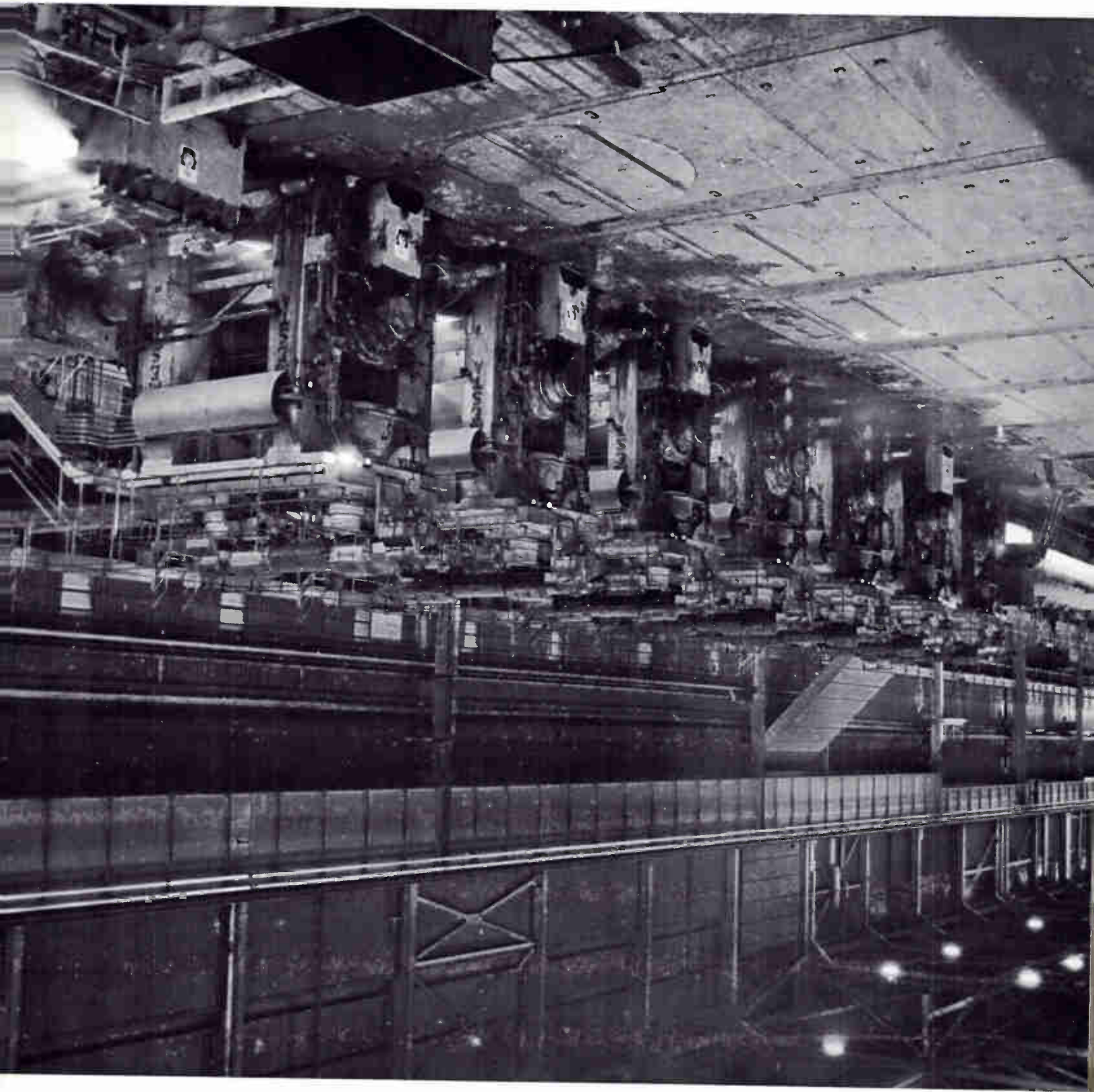
The determinations are made by use of programmed model equations and logic, which represent typical conditions in the mill, grade characteristics, slab size, and desired strip dimensions. The

equations and logic also predict the settings of the rolling equipment that should reduce an incoming slab of a particular grade to the desired product thickness and width. The settings must be determined for every variety of product to be rolled, they must give acceptable product quality, and they must be adjustable throughout the life of the installation because both conditions and requirements tend to change.

On the first computer-controlled mills, control adjustments were made by collecting data concerning each piece run through the mill and analyzing that data in another computer (or on the control computer when the mill was shut down) to determine what correction was required. That, however, is a time-consuming and expensive chore because of the volume of data available. A typical mill may run five passes through the roughing mill and seven through the finishing mill at a rate of about one coil a minute; more than 5000 sets of data concerning force, horsepower, and reduction can be collected during each 8-hour shift. It is obviously impossible to punch all that data into cards for the computer's analysis. Data must be selected, but the difficulty of deciding which data are relevant and representative is a serious complication.

Off-line analysis has the further disadvantage of requiring attentive checking to detect changes in grade, slab size, desired strip dimensions, and mill conditions. Then data have to be collected on the changes and analyzed to alter the model constants in such a way as to improve the mill setup predictions for the new conditions.

**Right**—These finishing stands are part of the computer-controlled hot strip mill at the Indiana Harbor Works, Youngstown Sheet and Tube Company. Heated slabs are first reduced in thickness by a roughing mill, and then the finishing mill further reduces the thickness to produce finished coils of hot-rolled strip. The 84-inch mill's control system employs an adaptive technique that enables the control computer to teach itself how steel must be rolled in that particular mill so as to produce the desired final strip dimensions from slabs of different sizes and grades.



To overcome those disadvantages, a type of adaptive control was developed by Westinghouse a few years ago. In it, the computer improved the mill settings as a succession of similar products was rolled. However, whenever grade or thickness changed, the computer had to discard the information collected and start over to make adjustments for the new product.

### *New Adaptive Control*

In the new adaptive control system, all experience is retained in the computer's memory and is applied selectively to slabs as they are received in the mill. As a new slab starts through the mill, the computer receives a punched card identifying the slab by its dimensions, grade, and desired finished strip dimensions. The computer checks its memory to determine if it has previously learned anything about that size and grade.

If material of that size and grade has never before been encountered by the computer, the equipment is set in accordance with the original model equation for that material. The first piece is then rolled. As the rolling proceeds, the computer receives information about the success of the original equation from sensors provided along the line. The information is stored in memory for use the next time that material is encountered.

*Rolling Stand Setup*—The most important mill control setting is the roll opening. Once the computer has determined the thickness to be delivered from each rolling pass, it must predict the roll separating force (caused by the entrance of steel) so that the roll opening can be so chosen as to compensate for the increase in the opening with separating force (the "mill spring"). The unloaded roll opening is called the "screwdown opening" because it is determined by the position of the motor-driven screw system used to position the upper roll.

The roll opening for a given pass is determined as shown in Fig. 1. The curves on the right represent the plastic deformation characteristic of the product being rolled, with the dashed curve being predicted characteristics and the solid curve actual. (Force increases as delivery

thickness decreases.) The curve on the left represents the mill spring characteristic; its slope is called the mill modulus. The screwdown opening shown is the roll separation at no load. The intersection of the plastic-deformation and mill-spring curves is the point at which the force exerted by the mill equals the force required to deform the product, so it is the point that determines the product thickness to be produced on that pass.

Precise mill setup is dependent on the calibration of the screwdown system, the repeatability of the mill modulus, and the predictability of the roll separating force required to make a certain reduction ("draft") on the particular product. The mill characteristics (calibration and modulus) are maintained by recalibration each time the rolls are changed, and by on-line recalibration employing data collected as the rolling proceeds.

*Recalibration After Roll Changing*—A mill's rolls are removed for regrinding once or twice during each shift, and new rolls are installed. The stand must then be recalibrated to assure the accuracy of screwdown-positioning and force-measuring systems. Under the new system, the recalibration is done by the computer.

When the computer system is initially installed, the mill modulus is carefully determined by driving the screwdown system together as the rolls are turning (with no product in the mill) and collecting roll force data. Each time the mill is recalibrated, the computer checks at least two points along the mill spring curve to make sure the apparent mill modulus (ratio of change in roll opening to change in separating force) agrees with the predetermined mill modulus (Fig. 2).

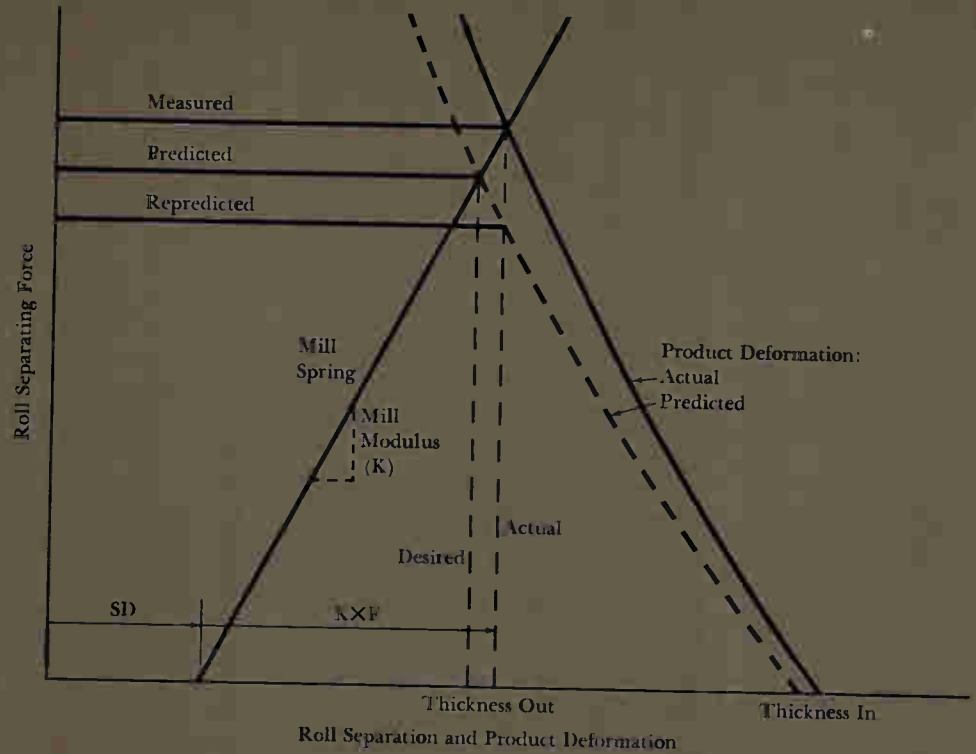
The rolls are driven together until a predetermined force is reached; while the rolls are kept at that initial position, the force is scanned and an average value (from at least ten force readings) determined. The rolls are then moved an additional distance together—say 0.050 inch—and the force measurements are repeated. The computer checks the change in force for this fixed change in screwdown setting to indicate the accuracy of the apparent mill modulus.

Within reasonable limits, the computer modifies roll separating force measurements as a result of this comparison of apparent and predetermined mill moduli. If the error is too large, an alarm is printed out and maintenance personnel are requested to check the roll force transducers.

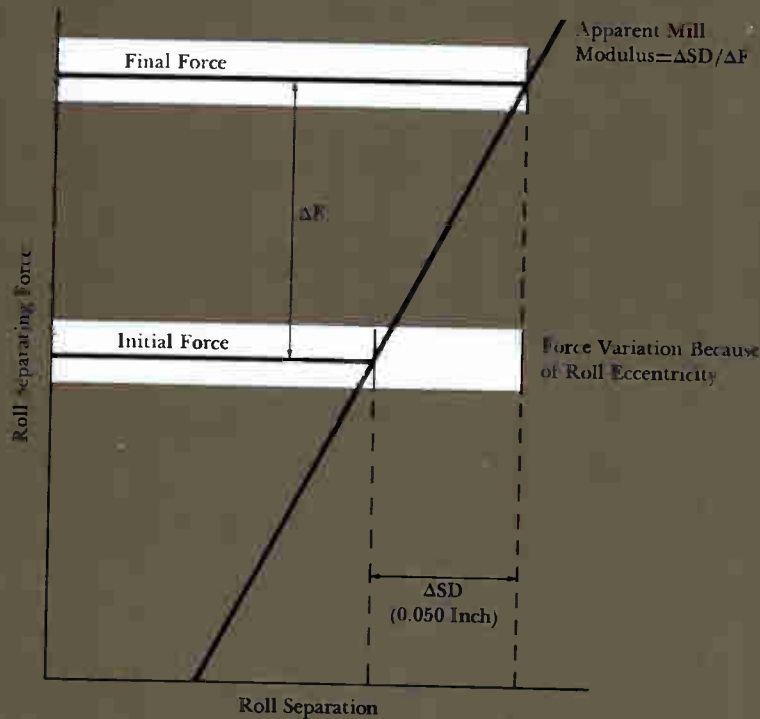
Because the rolls are not exactly round, variations in roll force are always present as the rolls turn. This eccentricity is measured by the computer during the recalibration procedure by detecting the variation in roll force each time the groups of force readings are taken. If the eccentricity is too great for good control of product thickness, the computer prints out an alarm.

*Recalibration During Rolling*—Screwdown systems on the finishing stands are continually calibrated as coils are rolled. The finished thickness from the last stand is measured by an X-ray thickness gauge and that reading, with the speeds of the other stands, is used to determine the gauge being delivered from each stand. (The principle is that mass flow rate must be constant throughout the mill.) By comparing this measured and calculated thickness with the thickness determined from measured roll force, screwdown position, and mill modulus, the computer determines the necessary adjustment to the screwdown calibration.

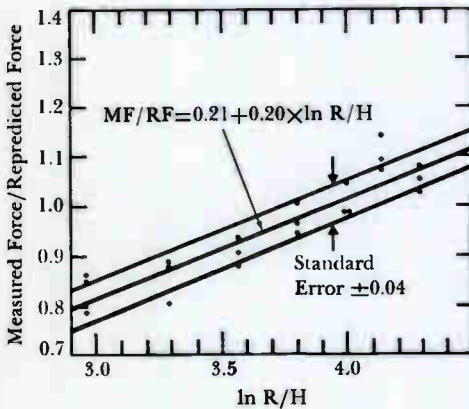
*Force Data During Rolling*—With well established and maintained mill characteristics, control of delivery thickness depends on good force predictions; consequently, a learning procedure is used to continually improve the roll force predictions. As rolling proceeds, a comparison between measured and predicted roll force is used to improve the mill settings. In the example shown in Fig. 1, the original predicted force is lower than the actual measured force, probably because the piece is cold. If force is repredicted by using the model equation for the actual draft taken, it is even lower than the original prediction because the higher force caused a smaller than expected reduction. A comparison of the measured and repredicted force is a true measure of the amount of correction needed in the model equation to match



1—The computer determines the thickness to be delivered from each rolling pass and then calculates the roll opening that will give the thickness. It starts with a model equation that predicts roll separating force ( $F$ ) as a function of product temperature, thickness in and out, tension, and grade; then it chooses the screwdown opening ( $SD$ ) that, with the mill spring caused by separating force, will produce the desired thickness out of the pass. As the rolling pass is made, roll separating force is measured and actual delivery thickness is determined by adding the mill spring ( $K \times F$ ) to the screwdown opening. ( $K$  is the mill modulus for that stand.) The computer then re-predicts separating force for the actual thickness and uses the ratio of the repredicted force divided into the measured force to improve force predictions in future rollings.



2—A mill stand's screwdown-positioning and force-measuring systems are recalibrated by the computer whenever the rolls are removed for surface grinding and replaced with fresh rolls. With no product in the mill and the rolls turning at normal speed, the rolls are driven together until a predetermined roll separating force is reached. The rolls are then moved an additional distance together (0.050 inch in this example) and the force change is measured. The ratio of the change in screwdown position ( $\Delta SD$ ) divided by change in roll separating force ( $\Delta F$ ), known as the apparent mill modulus, is compared with the well established mill modulus, and the roll separating force feedback signal is automatically adjusted.



3—For a reversing stand, the computer learns how to roll a new size and grade as illustrated in this example of three slabs rolled with seven passes each. The ratio of measured roll separating force divided by repredicted force was stored in the computer in the form of a linear equation as a function of the natural logarithm of  $R/H$ , where  $R$  is roll radius and  $H$  is entry thickness. (If the original model equation had done a perfect job, all of the points would have had a value of 1, but the roll separating force in this example was lower than predicted on the early passes and slightly higher than predicted on the later passes.) The computer will use the learned equation whenever a similar product is rolled in the future. Approximately 68 percent of the data is within the standard error, in this example  $\pm 0.04$ . The standard error is used to decide how good the data is and to test new data for reasonableness.

the measured value. The correction (ratio of measured force to repredicted force) is the value used in the learning procedure. It is a per-unit number that normally varies between 0.8 and 1.2 if the predictions are within 20 percent of the measurements. Corrections are checked for reasonableness before use.

As additional coils of the same hardness and thickness class are rolled, the data collected on each coil are used to continuously improve mill settings. When the size or type of steel in the mill changes, the information learned is stored in a learning table in computer memory for use when the same material appears again. The computer then chooses the appropriate information from the tables for the new material being rolled.

The learning procedure is made simple, reliable, and flexible by classifying the products being rolled so that the information learned is applied to a relatively narrow range of products. Most systems use at least five alloy classes and five slab thickness classes to describe the product spectrum in the roughing mill. Five or more additional classes should be established for product thickness from the finishing mill. Learned information then is used only for products within the range for which it was learned.

A system of weighting regulates the response rate of the control system (the rate at which mill adjustments are changed in response to variant measurements on any coil). The weighting depends on the number of times the computer has previously encountered the same material. Information learned on the first encounter causes a fairly large change in the mill setup for the second coil. However, after many coils of that class have been rolled, the measurements made on any one coil make only a small change in the settings for the next.

This sort of logic closely follows that used by a capable operator. The weighting-factor technique is shown in the following equation:

$$\text{New Mean} = \frac{\text{Old Mean} \times WF + \text{New}}{WF + 1}$$

where *mean* is the weighted mean value of

the correction, *new* is the new value to be added to the old mean value to determine a new mean value, and *WF* is the weighting factor.

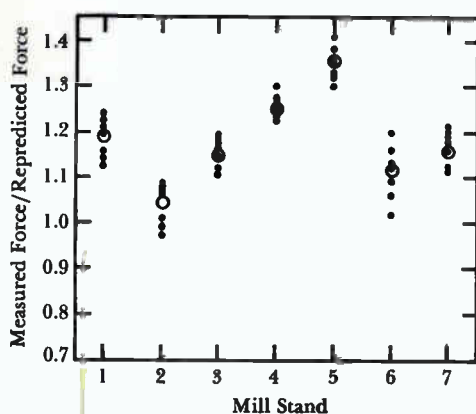
On the first coil rolled, the weighting factor is normally set to 0, and the new mean value used on the second coil is equal to the new value; the old mean is discarded. After the rolling of several coils, the weighting factor is increased, say to 5, causing the new mean to be 5/6 of the old mean plus 1/6 of the new. The larger the weighting factor, the slower the response to new information.

This same technique is used for the long-term learning, but the weighting factor is a larger number, such as 30, so that the learning table is representative of the rolling of many coils rather than just the last one.

*Reversing-Stand Learning Procedure*—The method used for storing the learned information for a reversing stand is shown in Fig. 3. A simple equation, in this case a first-order linear polynomial, represents the information to be learned—measured roll separating force divided by repredicted roll separating force. The equation is a function of the roll radius divided by the entry thickness at the particular pass. The figure shows information collected on three pieces rolled through the mill, each requiring seven passes.

If the model equation did a perfect job of predicting, the correction would be 1 for all thicknesses. In the example shown, however, as the thickness became less ( $R/H$  became greater), the measured force as compared to the repredicted force increased. This tendency to predict too high a force on the early passes and too low a force on the later passes was stored in the equation and used, whenever a similar product was rolled, to improve the predictions in accordance with the learning. The constants for the learning equation are determined by a least-squares fit, which minimizes the square of the error between the learning equation and the measured values.

The program also determines the standard error, which is a measure of how closely the equation matches the measured data. With a normal distribution of error,



4—For a tandem mill, the computer learns by calculating and storing the mean value, at each mill stand, of the ratio of measured roll separating force to re-predicted force. This example shows results from seven coils rolled in a seven-stand mill; solid dots show the force ratios, and open circles show the mean values. Whenever a similar product is rolled again, the stored mean values are used to improve the predictions of roll separating force to better control the mill settings.

the standard error includes about two-thirds of the measurements. The standard error is a useful piece of information in the program, which limit-checks each set of data to determine whether it is reasonable and useful for learning. Since the normal scatter of the data is known for that particular thickness and grade, a test is made to determine whether any particular set of data is within the normal distribution of error or whether it is probably erroneous because of its size compared with the standard error.

*Tandem-Mill Learning Procedure*—The method of storing learned values for a tandem mill is shown in Fig. 4. It has long been a frustration in developing the model equations for such a mill to note that the rolling characteristics in various stands of tandem mills seem to be quite different. In this particular mill, one explanation of the variation from stand to stand is that oil is sprayed on the rolls of stand 2, and some of it is carried on to later stands.

Regardless of the reason why, the model equation seems to predict in a rather erratic way on the various stands of the tandem mill. Since the error patterns are quite repeatable so long as the major conditions stay the same, such patterns are learned and stored for future rolling. The standard error (variation band) of the mean for each stand and for each grade and thickness class is also stored, and it is used in testing the validity of any set of data collected during rolling.

*Rolling Power Predictions*—Torque and horsepower requirements also are predicted. They are used to limit the draft taken in any pass, to divide the work among the various passes, and to determine the speed at which rolling can be done. The predicting and storing are done in much the same manner as for roll opening.

### Conclusion

The adaptive learning procedure is useful on any type of rolling mill, and it could be used in any other process control system in which predictability of the process variables can be assumed through classification. It substantially cuts the time

required to get the computer on line and producing quality product consistently by adjusting readily to changes in the characteristics of the incoming material and to new specifications for the finished product.

The weighting factor protects the control system from over-correction when one or more passes vary considerably from the normal, as is common in a reversing mill. And it allows for correction of seemingly erratic behavior in one or more stands if that behavior is encountered regularly.

The normal variation of data for the particular product as determined by the computer from previous rolling is used to determine whether the computer will accept the new correction or ignore it.

The new procedure also makes it possible for the operator to call for maintenance work before errors in sensing mechanisms become so serious as to detract from the quality of the products. Changes in mill characteristics, such as roll lubrication and other environmental variables, can be made without extensive manual retuning; when such changes occur, the weighting factors can be adjusted to respond quickly with corrected information.

Experience with both the Republic and the Youngstown mills indicates that the on-line adaptive programs are of more importance than the accuracy of the original model in determining the quality and consistency of the product rolled. Thus, a relatively simple model can be used to generate the original schedules and mill setups, and then the adaptive learning procedure gets the system functioning well with a minimum of complexity and off-line adjustment.

# Fast Valve Control Can Improve Turbine-Generator Response to Transient Disturbances

O. J. Aanstad  
H. E. Lokay

*The modern electrohydraulic turbine control system has the ability to rapidly close the turbine interceptor valves upon detection of a severe system fault. Computer studies have indicated that fast turbine valve control can improve unit stability, thereby increasing the critical fault clearing time.*

In the continuing effort to improve system reliability, the trend is to design power systems that will insure generating unit stability during severe faults or transient disturbances at or near the power plant. A "severe fault" could be a three-phase fault that is cleared in breaker-failure or backup-relay clearing times, accompanied by a reduction in transmission system capability following fault clearing.

At the same time that system performance criteria are becoming more severe, increasing electrical demand and utility company pooling of generating facilities are resulting in the installation of larger and larger rated units. Advances in turbine-generator design are leading to increased turbine element flow capabilities and improved generator cooling techniques—both tending to reduce unit weight per kilowatt of rating, and the latter resulting in higher generator electrical reactances. All these factors contribute to a reduction in the ability of the turbine-generator unit to remain in synchronism with the system following fault clearing.

To achieve the needed system stability, the system planner must understand and select from a variety of stability control techniques now available—fast-acting relay systems, high response excitation systems, rapid-clearing circuit breakers, independent circuit-breaker pole relay and operating systems, and reduced-reactance unit transformers. To this list should be added a new concept, *fast turbine-valve control*,<sup>1</sup> a technique that reduced turbine input power rapidly following recognition of a severe fault

condition, thereby reducing unit accelerating power and improving unit stability.

Fast turbine-valve control is made possible by the new Westinghouse electrohydraulic (EH) turbine control system,<sup>2</sup> which uses solid-state electronics, high fluid pressure in the hydraulic system, and new fast-response turbine valves. Since the newest large turbine-generator units with EH control use rapid turbine-valve control for overspeed protection following a full-load rejection, this same control system lends itself to unit stability control following severe system disturbances.

## Unit Transient Stability

The improvement in unit transient stability with fast valve control can be illustrated with the conventional power-angle diagram and the equal-area criteria for unit stability<sup>3</sup> (Fig. 1a). The turbine-generator unit and the power system are in balance at point *P* on the *before-fault* power-angle curve. When a fault occurs near the plant, generator electrical power output decreases to  $P_1$ , causing mechanical input power to greatly exceed electrical output power. The excess turbine power causes the unit to accelerate, increasing its angle ( $\theta_1$  to  $\theta_2$ ) relative to the system. When the fault is cleared the generator output power increases to  $P_2$  on the *post-fault* power angle curve. (The post-fault power angle curve is lower than the pre-fault curve because transmission lines have been opened to clear the fault.) The excess electrical output power over mechanical input power causes the unit to decelerate. If area *B* (Fig. 1a) is greater than area *A*, the generator stays in synchronism with the system. The initial power level and/or the fault clearing time for which areas *A* and *B* are equal is defined as the *transient stability limit*.

In Fig. 1a, the steam input to the turbine is assumed constant. Actually, since the unit accelerates during the fault, the increase in unit speed causes the turbine speed control to reduce turbine input power by reducing input steam. However, since the time involved when considering transient stability is only about one second, very little speed control action can occur. Input power is reduced

only slightly, but it is in the direction to improve unit stability, as shown in Fig. 1b by the slight increase in area *B*.

With fast turbine-valve control, turbine valves are closed as quickly as possible upon recognition of the fault and then opened slowly following a short time delay. Therefore, steam flow or input power is quickly reduced as shown in Fig. 1c. The significant increase in area *B*, and thus the increase in the transient stability limit, is readily apparent. Thus, for the same initial unit loading (input power), a longer fault duration can be permitted and still have the unit remain stable with the system.

## Dynamic Characteristics of Large Steam Turbines

The power response of a large steam turbine following a change in turbine-valve position is mainly a function of the valve flow-position characteristics, steam flow and steam conditions throughout the turbine, turbine internal volumes, and the power distribution between the different turbine elements.

A large steam turbine is equipped with four sets of valves, as shown in Figs. 2 and 3. The stop-throttle and reheat stop valves are primarily emergency trip valves and are not responsive to on-line speed and load variations; the main inlet control valves modulate steam flow through the turbine during normal load operation. Both inlet control and reheat interceptor valves are responsive to the overspeed protection controller (OPC) to limit overspeed following a complete sudden loss of electrical load.

## Fast Turbine-Valve Control

*Fossil-Fired Units*—The steam flow path through a modern fossil-fired, tandem-compound, single-reheat turbine-generator unit is shown in Fig. 2. Inlet steam enters the high-pressure turbine control

O. J. Aanstad is a controls development engineer at the Westinghouse Large Turbine Division, Lester, Pennsylvania; H. E. Lokay is Manager, Rotating Machinery-Generation, Power Systems Planning, Westinghouse Electric Corporation, East Pittsburgh, Pennsylvania.

1—Unit power angle curves illustrate the "equal area" transient stability concept ( $B \geq A$ ) for (a) constant input power to the turbine, (b) turbine speed control which decreases input power slightly, and (c) fast turbine-valve control which decreases input power significantly.

stage through the main inlet stop-throttle valves, the steam chests, the main inlet control valves, and the inlet piping. Reheat steam flows into the intermediate-pressure turbine through the reheat stop valves, the reheat interceptor valves, and the reheat inlet piping. Cross-over piping provides the steam path from the intermediate-pressure turbine exhaust to the low-pressure inlet flanges.

The main and reheat inlet features are separately mounted and anchored to the foundation to minimize the thermal-mechanical reaction forces acting on the turbine elements from the steam piping. However, this arrangement results in a relatively large volume of uncontrolled steam between the control valves and the high-pressure turbine and between the interceptor valves and the intermediate-pressure turbine.

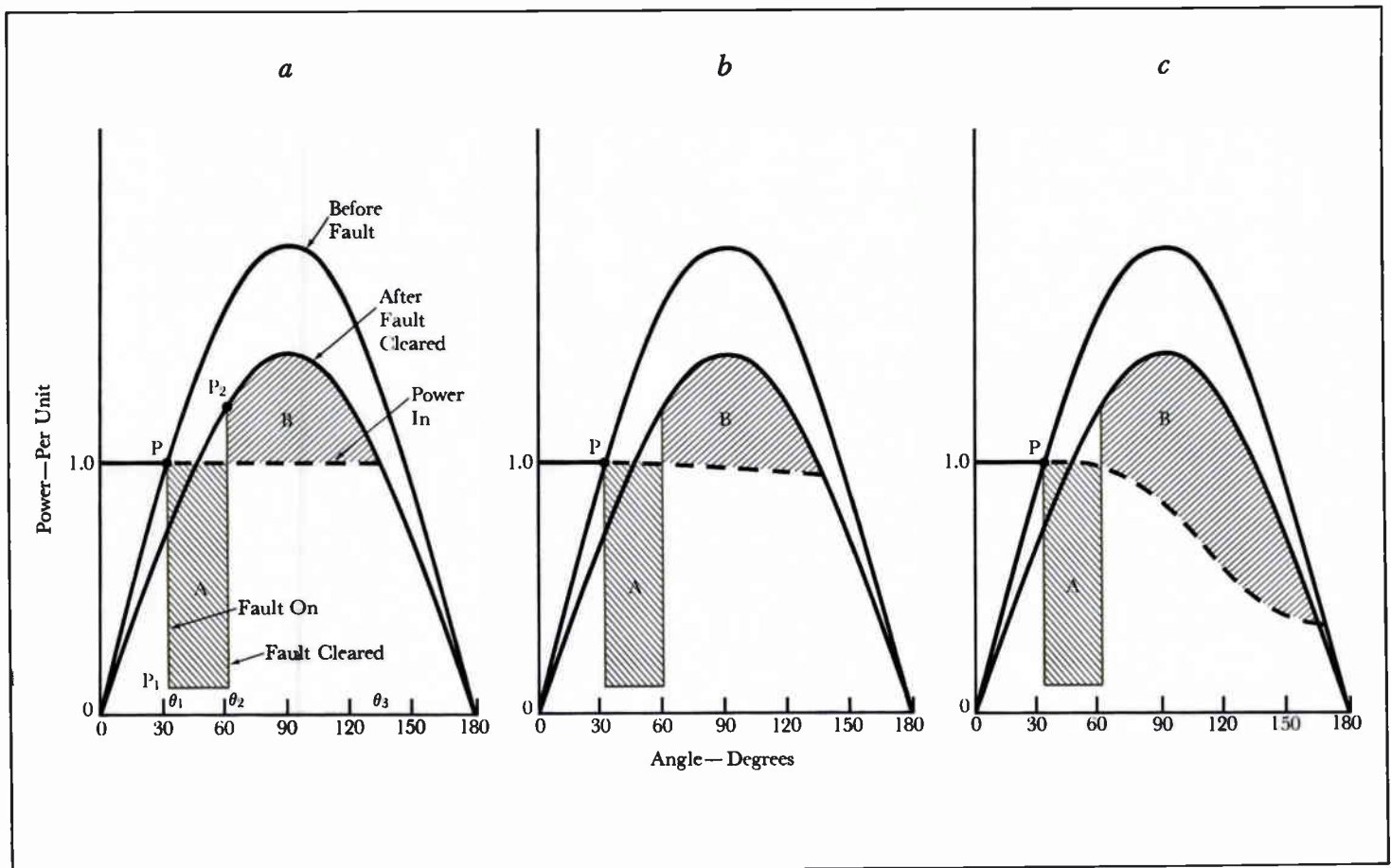
Feasibility studies show that the most practical way to reduce turbine power rapidly is to close *only the interceptor valves*. These valves control steam flow to the intermediate and low-pressure turbine elements, which in combination generate approximately 70 percent of the total unit power. By closing the interceptor valves, this major portion decays quickly because the stored energy effect of the reheater is avoided. This valving scheme is generally referred to as *fast turbine-valve control*.

When the interceptor valves close, the large reheat volume absorbs steam flow ahead of the interceptor valves for several seconds. This cushioning effect, along with possible blowing of reheat safety valves, minimizes the transient felt by the steam supply system. (However, in the event that reheat safety valves do open, reseating difficulties and resulting steam

leakage could cause operating problems.)

Although there are two other valve combinations that might be used for fast load control, they would not be as effective as operating just the interceptor valves. For example, closing the control valves and the interceptor valves would result in fast decay of high-pressure turbine power as well as intermediate- and low-pressure turbine power, but the abrupt shutoff of steam flow would impose a severe transient shock on the boiler and the boiler control systems; furthermore, the quick steam pressure increase could cause blowing of the boiler safety valves.

The third possible alternative, closing only the control valves, would have the bad feature of the above method. Besides, decay of intermediate- and low-pressure power would be slow because of the large





amount of entrapped steam in the reheater.

**Nuclear Units**—The steam flow path for a nuclear, tandem-compound, single-reheat turbine-generator unit is shown in Fig. 3. Main steam enters the high-pressure turbine through the main inlet stop-throttle valves, the steam chests, the main inlet control valves, and the inlet piping. The high-pressure exhaust steam passes through the moisture separator reheater and enters the low-pressure turbine through the reheat stop valves and the reheat interceptor valves.

As with a fossil-fired unit, closing just the interceptor valves is the best method of accomplishing fast load control. With nuclear turbines, the interceptor valves are located in the crossover piping close to the low-pressure inlet flanges, resulting in a smaller volume of uncontrolled reheat steam than in a fossil-fired unit and therefore better dynamic response.

#### Turbine Power Decay Following Fast Valving

Turbine power decay following a fast valving action is a function of response of the overspeed protection controller for load unbalance detection, interceptor valve closing time, interceptor valve flow-shutoff characteristic, and steam volumes and steam conditions downstream from the interceptor valves.

A load unbalance is detected by electrical transducers and solid-state electronics (see *Fast-Valving Logic*). An amplified electrical signal energizes solenoid valves, which in turn operate the hydraulic dump valves on the interceptor-valve actuators. This electrohydraulic approach minimizes control system dead time ( $T_D$ ).

Valve actuator closing times are presently in the range of 0.15 to 0.2

2—The steam flow path and valving is shown for a fossil-fired turbine-generator unit. The overspeed protection controller compares turbine power input with generator output and provides a control signal for fast valving.

3—Steam flow path and valving is shown for a nuclear turbine-generator unit. An overspeed protection controller is applied the same as shown in Fig. 2.

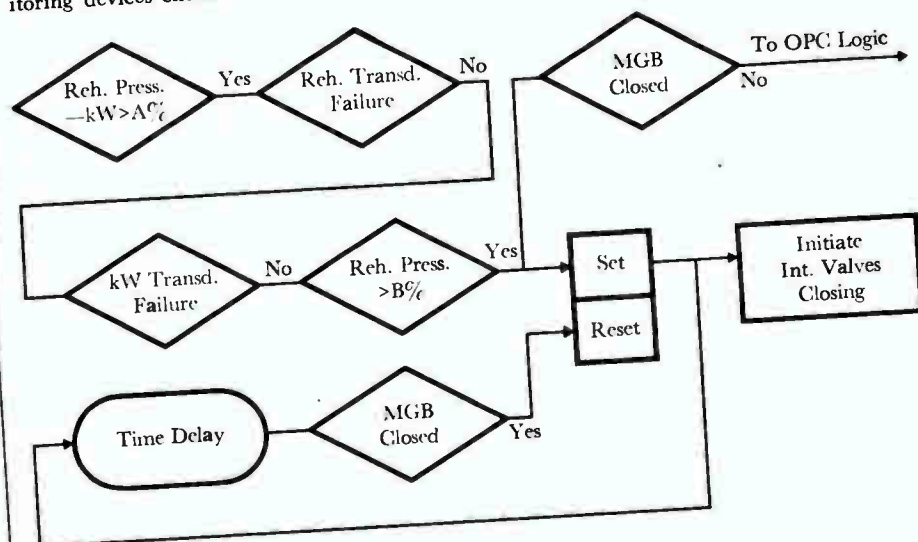
#### Fast-Valving Logic

The new Westinghouse overspeed protection controller with the fast-valving feature measures mechanical power input to the generator with a pressure transducer connected to a stage pressure downstream from the reheater; electrical power output from the generator is measured with a Hall watt transducer. Under steady-state conditions, reheat pressure is proportional to electrical output so that the signals to the overspeed protection controller are in balance. A mismatch occurs when electrical power is suddenly lost, and control system response is initiated.

As shown in the diagram, control response is initiated (yes) when reheat pressure exceeds electrical output by a preset quantity ( $A$  percent). Two following monitoring devices check each transducer to be

sure that neither has failed (no). And finally, if reheat pressure is greater than  $B$  percent (adjustable), a control signal is generated for two purposes:

- 1) If the main generator breaker (MGB) is open, the signal activates the turbine overspeed protection controller (OPC) to close both the control and the interceptor valves.
- 2) If the main generator breaker is closed, indicating a partial system load loss, fast valving (closing of the interceptor valves only) is initiated. The closing signal also initiates a time delay (adjustable) so that if the turbine-generator unit remains tied to the system (MGB closed), the logic is reset, removing the closing signal from the interceptor valves to allow them to re-open slowly.



nisms for each pole with timing control capable of closing the contacts accurately with respect to the voltage of each phase.

For a breaker without any resistors, the computer study showed that, to limit the surges to 1.5 per unit, each breaker pole must close within  $\pm 1.0$  msec of the instant of minimum voltage across the contacts. With a tolerance of  $\pm 1.5$  msec, a maximum voltage surge of 1.7 per unit was obtained, and, with  $\pm 2.0$  msec, over-voltages of 2.0 per unit occurred. These tight tolerances, the necessity of measuring both line and source side potentials, and control problems make this approach unattractive compared to other alternatives.

A very effective arrangement for that breaker type, however, is the use of two resistance steps with less tightly controlled closing. It was found that the insertion of 1500 ohms for at least 6 msec, followed by a reduction to 300 ohms for another 6 msec, could take place at random with respect to the system voltage without producing surges over 1.5 per unit, provided that the 1500-ohm resistance in all phases was inserted prior to introduction of any of the 300-ohm sections. However, to limit the final transient occurring when all the resistance is shorted out (closing of contact C of Fig. 1) to 1.5 per unit, this closure must occur within  $\pm 2.5$  msec of voltage zero across the 300-ohm resistor. This is a reasonable tolerance for well-designed modern operating mechanisms such as are used in the Westinghouse EHV circuit breaker.

Controlled closing is accomplished by circuitry that uses a low-voltage signal in phase with the bus voltage to produce a pulse at each voltage zero. This signal is the input to a switch that acts as a gate for the external closing command. Whenever the switch is made conducting, a pulse is fed into an adjustable time delay element whose output energizes the breaker closing coil. The delay element is adjusted to provide the desired instant of main contact closure, taking into account the closing time of the breaker and allowing for the phase displacement between the bus voltage zero and the 300-ohm resistor voltage zero. Similar circuitry is provided for each pole. Means can be

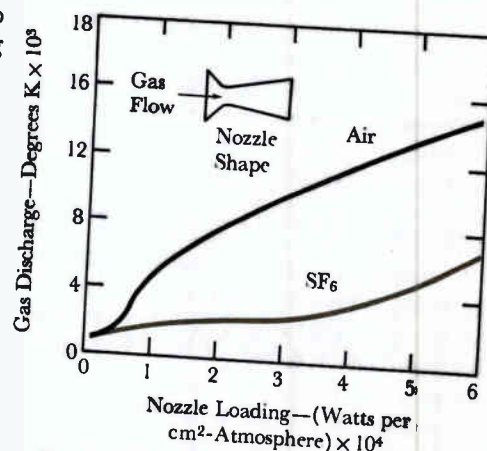
incorporated in the delay element to compensate for the variation in closing time with ambient temperature, pressure, and control voltage. These effects are minimized by suitable modifications in breaker design such as low-friction bearings where required.

According to statistical principles, the spread of closing times should show a standard deviation of not more than 25 electrical degrees to assure that the required 2.5-millisecond (54 degrees) tolerance is met 98 percent of the time. Timing tests on this type of breaker have indicated the feasibility of obtaining such a level of performance quite easily.

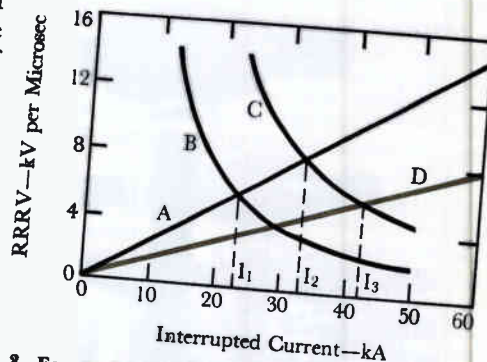
### SF<sub>6</sub> for Arc Interruption

Air-blast breakers, unlike SF<sub>6</sub> breakers, require separate resistors for the opening mode to limit the rate of rise of recovery voltage (RRRV). Moreover, comparisons of the best designs of EHV air-blast and SF<sub>6</sub> circuit breakers indicate that air-blast breakers require approximately four times the gas pressure of the SF<sub>6</sub> breakers to provide only about half the voltage recovery rate under a severe short-line fault condition. Therefore, the inherent capability of SF<sub>6</sub> for quenching high-current arcs is about eight times the inherent ability of compressed air. This striking difference is generally described in terms of an arc time constant for the deionization process at the moment of arc current zero. In highly effective SF<sub>6</sub> interrupters, this time constant can be as small as a fraction of a microsecond, compared with several microseconds for compressed air. The complex phenomena underlying these observed differences in performance are now being understood better by the use of new analytical approaches aided by modern computers.

The favorable physical, chemical, and electrical properties of SF<sub>6</sub> are: (1) a wide useful range of temperatures and pressures in the vapor state, (2) good heat transfer ability, (3) nontoxicity and chemical stability up to at least 150 degrees C, and (4) the highest dielectric strength of any commercially available gas suitable for arc interruption. Furthermore, the symmetry and bond strengths of the SF<sub>6</sub> molecule yield high-temperature proper-



2—Curves obtained from computer simulation illustrate the interrelation of various breaker parameters. For one particular nozzle shape, gas-blast nozzle loading (watts arc power divided by square centimeter throat area times absolute atmospheres pressure at the throat) is compared with the mean discharge temperatures for air and SF<sub>6</sub>. The gases are flowing at their sonic velocities through the nozzle, which contains a uniformly distributed arc. SF<sub>6</sub> is clearly superior in its ability to carry away energy with a lower temperature rise.



3—For a short line fault, the relationship between the rate of rise of recovery voltage (RRRV) and the interrupted current for the system is shown as curve A from the equation  $RRRV = \sqrt{2}\omega Z I \times 10^{-4}$ . The capability of the interrupter, from the equation  $RRRV = K_1 P^{1.25} / I^{1.5}$ , is shown as curve B. By varying the parameters involved, this curve can be shifted to the right as in curve C, thereby increasing the interruption rating from  $I_1$  to  $I_2$ . If two breaks are used in series, the system RRRV per break can be reduced (curve D) to further improve the interruption rating to  $I_3$ .

amount of entrapped steam in the reheater.

**Nuclear Units**—The steam flow path for a nuclear, tandem-compound, single-reheat turbine-generator unit is shown in Fig. 3. Main steam enters the high-pressure turbine through the main inlet stop-throttle valves, the steam chests, the main inlet control valves, and the inlet piping. The high-pressure exhaust steam passes through the moisture separator reheater and enters the low-pressure turbine through the reheat stop valves and the reheat interceptor valves.

As with a fossil-fired unit, closing just the interceptor valves is the best method of accomplishing fast load control. With nuclear turbines, the interceptor valves are located in the crossover piping close to the low-pressure inlet flanges, resulting in a smaller volume of uncontrolled reheat steam than in a fossil-fired unit and therefore better dynamic response.

#### Turbine Power Decay Following Fast Valving

Turbine power decay following a fast valving action is a function of response of the overspeed protection controller for load unbalance detection, interceptor valve closing time, interceptor valve flow-shutoff characteristic, and steam volumes and steam conditions downstream from the interceptor valves.

A load unbalance is detected by electrical transducers and solid-state electronics (see *Fast-Valving Logic*). An amplified electrical signal energizes solenoid valves, which in turn operate the hydraulic dump valves on the interceptor-valve actuators. This electrohydraulic approach minimizes control system dead time ( $T_D$ ).

Valve actuator closing times are presently in the range of 0.15 to 0.2

2—The steam flow path and valving is shown for a fossil-fired turbine-generator unit. The *overspeed protection controller* compares turbine power input with generator output and provides a control signal for fast valving.

3—Steam flow path and valving is shown for a nuclear turbine-generator unit. An overspeed protection controller is applied the same as shown in Fig. 2.

#### Fast-Valving Logic

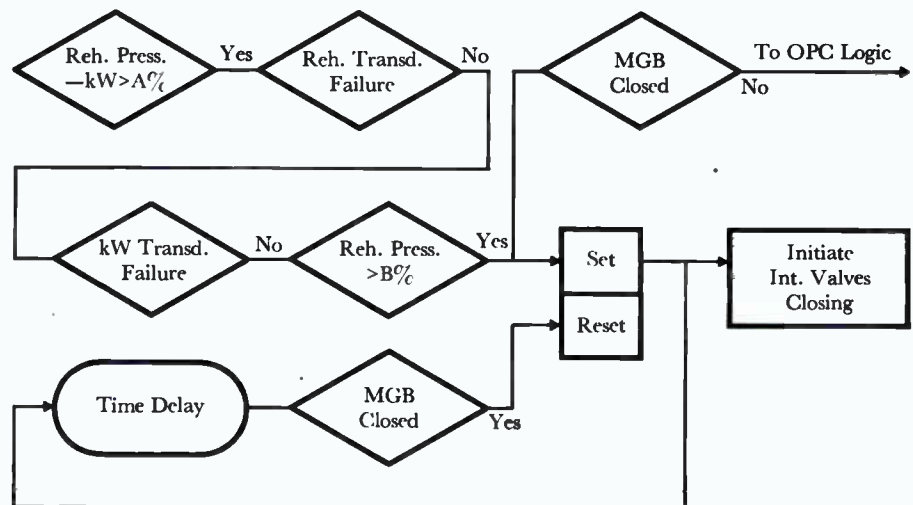
The new Westinghouse *overspeed protection controller* with the fast-valving feature measures mechanical power *input* to the generator with a pressure transducer connected to a stage pressure downstream from the reheater; electrical power *output* from the generator is measured with a Hall watt transducer. Under steady-state conditions, reheat pressure is proportional to electrical output so that the signals to the overspeed protection controller are in balance. A mismatch occurs when electrical power is suddenly lost, and control system response is initiated.

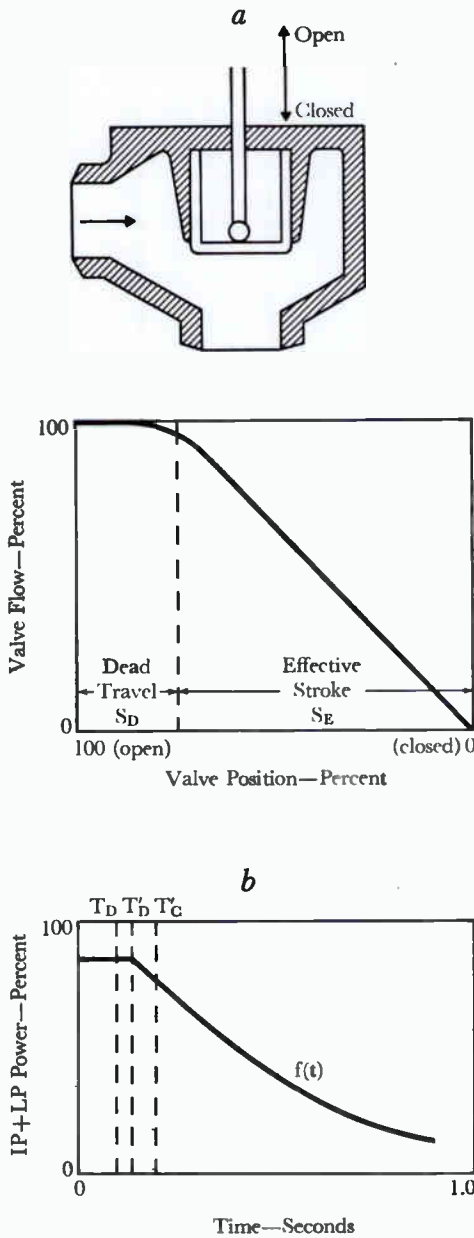
As shown in the diagram, control response is initiated (*yes*) when reheat pressure exceeds electrical output by a preset quantity ( $A$  percent). Two following monitoring devices check each transducer to be

sure that neither has failed (*no*). And finally, if reheat pressure is greater than  $B$  percent (adjustable), a control signal is generated for two purposes:

1) If the main generator breaker (*MGB*) is open, the signal activates the turbine overspeed protection controller (*OPC*) to close both the control and the interceptor valves.

2) If the main generator breaker is closed, indicating a partial system load loss, fast valving (closing of the interceptor valves only) is initiated. The closing signal also initiates a time delay (adjustable) so that if the turbine-generator unit remains tied to the system (*MGB closed*), the logic is reset, removing the closing signal from the interceptor valves to allow them to re-open slowly.





4—(a) The plug-type interceptor valve used with fossil-fired units requires some dead travel ( $S_D$ ) before the effective stroke ( $S_E$ ) begins. The resulting dead time ( $T'_D$ ) and the effective closing time ( $T'_C$ ) are shown with the IP + LP power decay curve  $f(t)$  for a fossil-fired unit (b) following a fast-valving action.

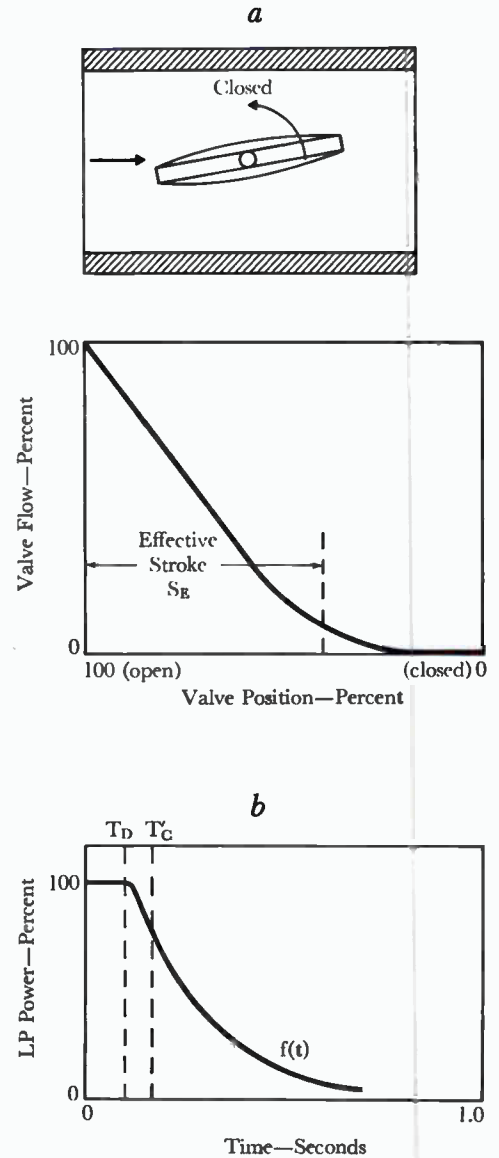
second including the dashpot part of the stroke. In this short interval, the moving masses (equivalent to the mass of an automobile) are accelerated from standstill to maximum velocity and decelerated to an acceptable impact speed before striking the valve seat.

The valve flow-shutoff characteristic depends on the type of interceptor valve used. The plug-type interceptor valves applied to fossil-fired machines must close 15 to 25 percent of their total stroke from the wide-open position before effective steam throttling begins (Fig. 4a). A typical intermediate-pressure plus low-pressure turbine power decay curve for a fossil-fired unit following a fast valving action is shown in Fig. 4b; it shows the influences of control system dead time ( $T_D$ ), valve travel dead time ( $T'_D$ ), effective valve closing time ( $T'_C$ ), and expansion of entrapped steam  $f(t)$ .

The fast-valving technique is more effective with nuclear units than with fossil-fired units because the interceptor valves are located right at the low-pressure turbine inlet, thus minimizing the amount of uncontrolled steam. Furthermore, the interceptor valve is a butterfly type, which has a better flow-shutoff characteristic because effective throttling occurs at the beginning of the stroke from the wide-open position (Fig. 5a), reducing the effective stroke ( $S_E$ ) to about half the total stroke. And finally, the low-pressure steam condition minimizes the amount of entrapped steam energy in the low-pressure turbine itself. A typical low-pressure power decay curve for a nuclear unit following a fast valving action is shown in Fig. 5b.

**Gains in Transient Stability**

Detailed digital computer stability programs<sup>4</sup> that include the dynamic behavior of large steam turbines have been used to measure the gains in system transient stability when fast turbine-valve control is applied. In general, the gain is measured in increased cycles of critical fault clearing times. Control system dead time ( $T_D$  in Figs. 4b and 5b) is important in enhancing stability because it determines the time required for initiating valve closure after the fault begins. The



5—The butterfly-type interceptor valve (a) used with nuclear units provides improved valving action because the effective stroke ( $S_E$ ) begins immediately with valve movement, avoiding valve travel dead time ( $T'_D$ ). The effective stroke ( $S_E$ ) is reduced to about half the total stroke. In addition, the low-pressure power decay for a nuclear unit following a fast valving action is faster because interceptor valves are located at the low-pressure turbine inlet and steam conditions also minimize the amount of entrapped steam energy.

minimum value for  $T_D$  is approximately 0.1 second, a value that includes only direct sensing of load unbalance greater than the specified setting (30 to 100 percent unbalance) with no added time delays for determining location, type of fault, or if the fault will be cleared in primary or backup relay times.

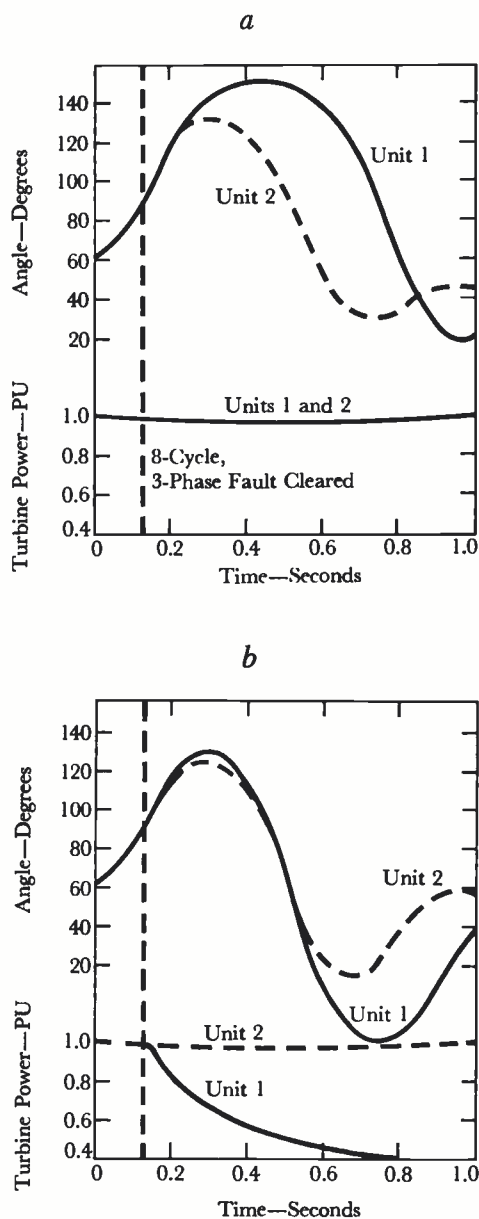
Unit swing curves obtained by computer study for two units in a two-unit plant that experience an eight-cycle, three-phase, high-side line fault are shown in Fig. 6. The units are seen to be stable with the system following a severe swing. Fast turbine-valve control is *not used* in Fig. 6a, and only a minor response from the turbine speed control is obtained. In Fig. 6b, one of the two units (machine 1) has fast valve control to initiate interceptor valve closing. Control system dead time ( $T_D$ ) is 0.1 second, but since the machines are fossil units, power decay does not start for 0.15 second. The maximum angle swing of unit 1 is significantly reduced by the fast-valving technique, and the angle swing for unit 2 is also somewhat lower. Although not shown here, other study results indicate that critical fault clearing time is improved by approximately one cycle when fast valve control is applied to only one unit, and by about two cycles when applied to both units.

Typical increases in critical fault clearing times for fossil units are one to two cycles. For nuclear units with higher unit inertias (larger H constants) and with turbine power decay starting slightly earlier ( $T'_D \approx 0$ ), an increase of two to three cycles may be expected. If additional time delay is required to define the fault or disturbance characteristics (increasing  $T_D$ ), the gains are decreased. For example, a three- to four-cycle delay reduces the gain by about one cycle.

### Conclusions

Fast turbine valve control is an economical and feasible way to enhance generating-unit stability. Closing only the interceptor valves provides the best overall solution for unit stability control.

The inherent dynamic characteristics of large steam turbine-generators limit the gain in stability improvement. Typical



6—Effect of fast turbine-valve closing on generator angle swing: (a) no fast valving on either unit, and (b) fast valving on unit 1.

gains in critical fault clearing times are one to two cycles for fossil units and approximately two to three cycles for nuclear units. For maximum gain, all units in the power plant should have fast turbine-valve control.

Additional time delay to define fault or disturbance characteristics before initiating valve closure greatly reduces the stability gains. It is possible to identify approximate fault severity by initiating valve closure by the unbalance power requirement setting (30 to 100 percent); however, considerable gain is lost if it is necessary to identify primary or backup cleared faults.

The application of fast turbine-valve control is new and field experience has not been obtained. Several units with this feature have recently been installed and several more are planned. Total performance evaluation is required through field testing to verify power decay curves, possible added valve maintenance, and performance of reheater safety valves. Field tests are being planned by several of the initial users in the near future.

### REFERENCES:

- <sup>1</sup>O. J. Aanstad, "Role of Prime Movers in System Stability—Dynamic Response and Data Constants for Large Steam Turbines," IEEE Winter Power Meeting, New York, 1970.
- <sup>2</sup>E. G. Noyes and M. Birnbaum, "Electro-Hydraulic Control Improves Operation and Availability of Large Steam Turbines," *Westinghouse ENGINEER*, March 1966, pp. 49-54.
- <sup>3</sup>*Electrical Transmission and Distribution Reference Book*, Chap. 13, Westinghouse Electric Corporation, Pittsburgh, Pa.
- <sup>4</sup>C. J. Baldwin and R. T. Byerly, "Improved Digital Simulation for Analyzing Power System Disturbances," *Westinghouse ENGINEER*, July 1969, pp. 109-16.

# New Goals for EHV and Future UHV Power Circuit Breakers

W. M. Leeds  
R. E. Friedrich  
T. E. Browne, Jr.  
C. L. Wagner

*High-voltage sulfur-hexafluoride circuit breakers are now being built to meet the difficult requirements of EHV and UHV power systems. Modular breaker construction can be provided to limit switching transients within 2.0, 1.7, or 1.5 per unit of normal crest voltage. Performance can be further improved by the addition of shunt capacitance on the line side of the breaker.*

The features of EHV transmission lines that attract public attention are the giant towers supporting great spans of bundled conductors on long insulator strings, with particularly spectacular construction where wide rivers are spanned. More important, however, are the problems of insulator contamination, ice loading, radio influence voltage, lightning and switching surges, system stability, and the reliability of the system interconnections under emergency conditions.

The power circuit breakers at the line terminals, which are often taken for granted, are now being asked to perform even more difficult tasks than ever before. New approaches to switching surge control make possible substantial cost savings in EHV line insulation, and the application of research on sulfur hexafluoride ( $\text{SF}_6$ ) arc quenching characteristics extends fault interrupting capabilities of the circuit breakers without resorting to extreme gas pressures or a large number of series contact breaks.

## Switching Surge Control

The insulation level of transmission lines rated 345 kV and below has been based primarily on lightning surge considerations. The attainment of 500-kV systems made switching surges the predominant factor, and circuit breakers employing single-step preinsertion resistors were developed to limit switching surges to

approximately twice normal crest voltage. Although the first 765-kV circuit breakers are being designed to this same switching surge level, new studies show that, to keep the line insulation down to the lightning level at system voltages above 500 kV, further reductions in switching surge magnitudes may be indicated. At 765 kV, for example, maximum switching surge levels of 1.7 per unit may be required, and 1100-kV (UHV) systems may need levels of 1.5 per unit or lower. (EHV ranges from 345 through 765 kV, and UHV from 1100 through 1500 kV.) New concepts of breaker design and operation are necessary to achieve these levels.

A Westinghouse EHV circuit breaker is shown in the photograph. Two interrupter modules with two contact breaks in each are provided for each of the three poles, with all modules mechanically operated by one pneumatic mechanism. The arc is quenched by a blast of high-pressure  $\text{SF}_6$  gas at each contact gap when the breaker is opened. Recent developments have made it possible, with some increase in dimensions, to rate such a design at 550 kV.<sup>1</sup> A breaker with three modules per pole, rated 765 kV and now under construction for the AEP system, will be the first circuit breaker of American manufacture to be installed at that voltage.

To determine the parameters required in a breaker to reduce switching surges to less than 2.0 per unit, a model system study was performed on the transient network analyzer (ANACOM).<sup>2</sup> The basic system configuration consisted of a 180-mile 500-kV bundle-conductor line connected through a well-grounded transformer and source ( $X_0/X_1=1.0$ ). The source impedance was varied to obtain the maximum transient overvoltage. Typical fault conditions were simulated by assuming all breaker operations to be reclosing against a trapped charge on the transmission line of 1.2 per unit on one phase and 1.0 per unit on the other two.

The computer study was performed for five different types of circuit breaker designs. For one group it was assumed that the contacts of all three poles closed substantially simultaneously, although the

energizing of the close coil was on a random time basis—that is, the contacts could close at any point on the system voltage wave.

When that type was used with no resistors, a maximum switching surge of 3.9 per unit was measured on the computer. With a 450-ohm resistor inserted in the circuit for approximately 6 msec and then shorted out by closing the main contacts, the maximum switching surge voltage produced was 2.05 per unit.

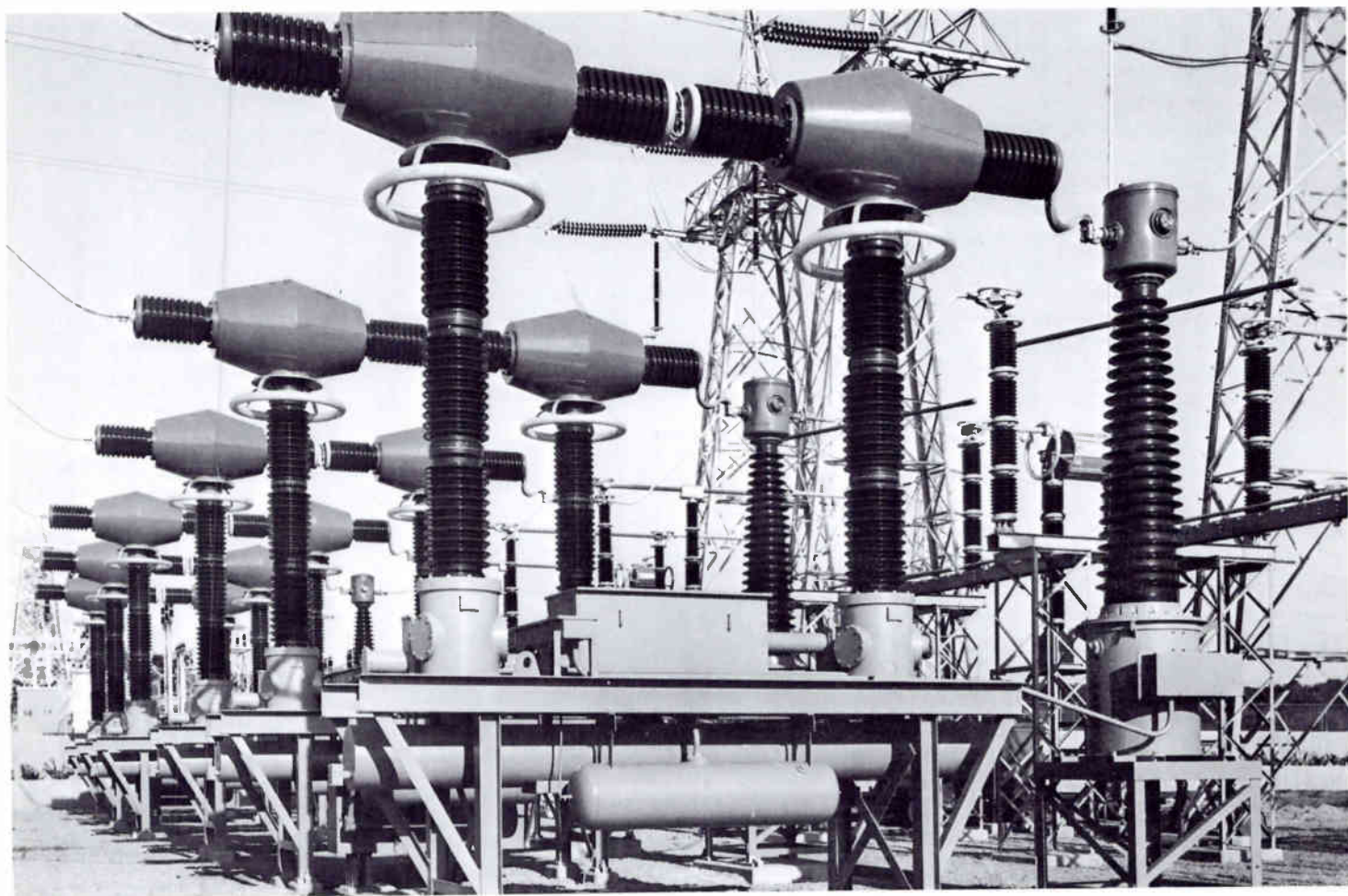
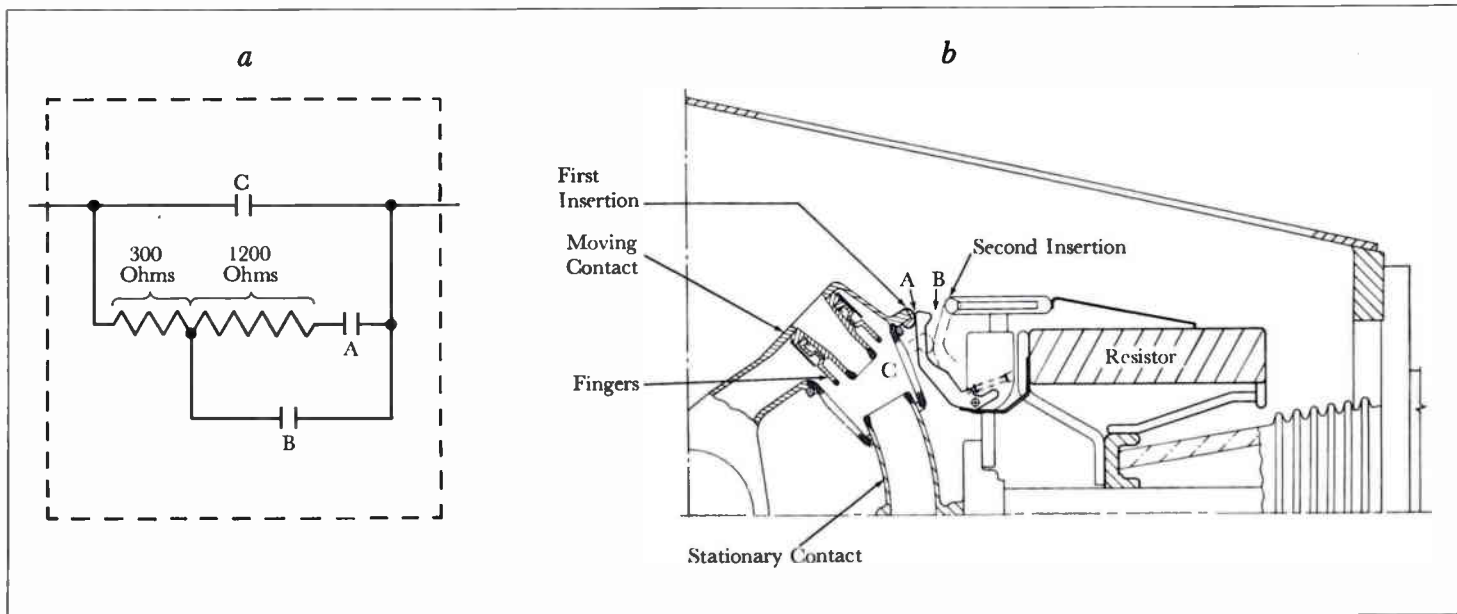
Fig. 1 shows two-step resistor insertion. When contacts *A* initially close, 1500 ohms of resistance per pole is connected. After a suitable time interval, contacts *B* close, shorting out 1200 ohms and leaving 300 ohms in the circuit. When the main contacts *C* close, all of the resistance is shorted out. The ANACOM showed that, by using a minimum insertion time of 10 msec for the 1500-ohm resistance, a minimum insertion time of 8 msec for the 300-ohm resistance, and a maximum pole span (range of contact closing times among the three phases) of 5 msec, the surges could be limited to 1.7 per unit.

The next group of breaker designs studied involves separate closing mecha-

1—Two-step resistor insertion used to limit surges is shown schematically (a) for an EHV circuit breaker. On closing, contacts *A* first meet, inserting 1500 ohms of resistance per pole into the circuit. Contacts *B* next close, shorting out 1200 ohms and leaving 300 ohms in the circuit. When the main contacts *C* close, all of the resistance is shorted out. The quarter cross section of a breaker module (b) illustrates the switching action. The tip of the moving contact arm picks up a hinged resistor contact, inserting the full resistance (*A* closes), after which contact is made to another resistor terminal that shorts out part of the resistor (*B* closes). Finally the fingers close around the stationary contact (*C* closes) and all resistance is shorted out. When opening, the resistor contact lags behind the rapidly accelerating moving contact, interrupting power without any resistance in the circuit.

Photo—Use of  $\text{SF}_6$  gas in EHV power circuit breakers such as these 345-kV units of Texas Power and Light provides for efficient and reliable interruption of short circuits. Each interrupter module contains two contact breaks, and there are two modules for each phase.

W. M. Leeds is Consulting Engineer, Power Circuit Breaker Division, Westinghouse Electric Corporation, Trafford, Pennsylvania. R. E. Friedrich is Manager, New Products Engineering, and T. E. Browne, Jr., is Long Range Major Development Section Manager, Power Circuit Breaker Division. C. L. Wagner is Manager, Transmission Control and Protection, Power Systems Planning, Westinghouse Electric Corporation, East Pittsburgh, Pennsylvania.



nisms for each pole with timing control capable of closing the contacts accurately with respect to the voltage of each phase.

For a breaker without any resistors, the computer study showed that, to limit the surges to 1.5 per unit, each breaker pole must close within  $\pm 1.0$  msec of the instant of minimum voltage across the contacts. With a tolerance of  $\pm 1.5$  msec, a maximum voltage surge of 1.7 per unit was obtained, and, with  $\pm 2.0$  msec, over-voltages of 2.0 per unit occurred. These tight tolerances, the necessity of measuring both line and source side potentials, and control problems make this approach unattractive compared to other alternatives.

A very effective arrangement for that breaker type, however, is the use of two resistance steps with less tightly controlled closing. It was found that the insertion of 1500 ohms for at least 6 msec, followed by a reduction to 300 ohms for another 6 msec, could take place at random with respect to the system voltage without producing surges over 1.5 per unit, provided that the 1500-ohm resistance in all phases was inserted prior to introduction of any of the 300-ohm sections. However, to limit the final transient occurring when all the resistance is shorted out (closing of contact C of Fig. 1) to 1.5 per unit, this closure must occur within  $\pm 2.5$  msec of voltage zero across the 300-ohm resistor. This is a reasonable tolerance for well-designed modern operating mechanisms such as are used in the Westinghouse EHV circuit breaker.

Controlled closing is accomplished by circuitry that uses a low-voltage signal in phase with the bus voltage to produce a pulse at each voltage zero. This signal is the input to a switch that acts as a gate for the external closing command. Whenever the switch is made conducting, a pulse is fed into an adjustable time delay element whose output energizes the breaker closing coil. The delay element is adjusted to provide the desired instant of main contact closure, taking into account the closing time of the breaker and allowing for the phase displacement between the bus voltage zero and the 300-ohm resistor voltage zero. Similar circuitry is provided for each pole. Means can be

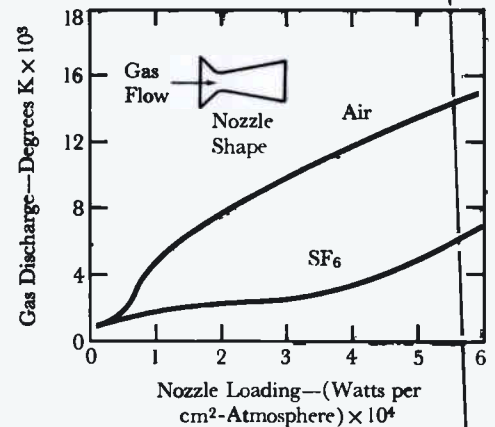
incorporated in the delay element to compensate for the variation in closing time with ambient temperature, pressure, and control voltage. These effects are minimized by suitable modifications in breaker design such as low-friction bearings where required.

According to statistical principles, the spread of closing times should show a standard deviation of not more than 25 electrical degrees to assure that the required 2.5-millisecond (54 degrees) tolerance is met 98 percent of the time. Timing tests on this type of breaker have indicated the feasibility of obtaining such a level of performance quite easily.

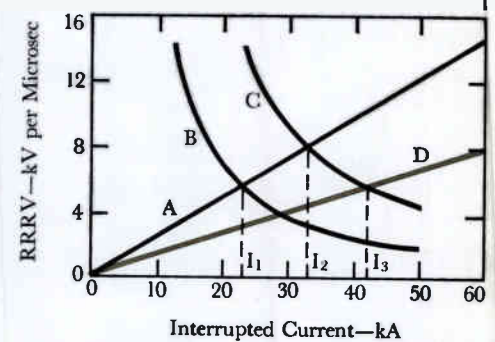
#### *SF<sub>6</sub>* for Arc Interruption

Air-blast breakers, unlike SF<sub>6</sub> breakers, require separate resistors for the opening mode to limit the rate of rise of recovery voltage (RRRV). Moreover, comparisons of the best designs of EHV air-blast and SF<sub>6</sub> circuit breakers indicate that air-blast breakers require approximately four times the gas pressure of the SF<sub>6</sub> breakers to provide only about half the voltage recovery rate under a severe short-line fault condition. Therefore, the inherent capability of SF<sub>6</sub> for quenching high-current arcs is about eight times the inherent ability of compressed air. This striking difference is generally described in terms of an arc time constant for the deionization process at the moment of arc current zero. In highly effective SF<sub>6</sub> interrupters, this time constant can be as small as a fraction of a microsecond, compared with several microseconds for compressed air. The complex phenomena underlying these observed differences in performance are now being understood better by the use of new analytical approaches aided by modern computers.

The favorable physical, chemical, and electrical properties of SF<sub>6</sub> are: (1) a wide useful range of temperatures and pressures in the vapor state, (2) good heat transfer ability, (3) nontoxicity and chemical stability up to at least 150 degrees C, and (4) the highest dielectric strength of any commercially available gas suitable for arc interruption. Furthermore, the symmetry and bond strengths of the SF<sub>6</sub> molecule yield high-temperature proper-



2—Curves obtained from computer simulation illustrate the interrelation of various breaker parameters. For one particular nozzle shape, gas-blast nozzle loading (watts arc power divided by square centimeter throat area times absolute atmospheres pressure at the throat) is compared with the mean discharge temperatures for air and SF<sub>6</sub>. The gases are flowing at their sonic velocities through the nozzle, which contains a uniformly distributed arc. SF<sub>6</sub> is clearly superior in its ability to carry away energy with a lower temperature rise.



3—For a short line fault, the relationship between the rate of rise of recovery voltage (RRRV) and the interrupted current for the system is shown as curve A from the equation  $RRRV = \sqrt{2}\omega ZI \times 10^{-6}$ . The capability of the interrupter, from the equation  $RRRV = K_1 P^{1.25} / P^{1.6}$ , is shown as curve B. By varying the parameters involved, this curve can be shifted to the right as in curve C, thereby increasing the interruption rating from  $I_1$  to  $I_2$ . If two breaks are used in series, the system RRRV per break can be reduced (curve D) to further improve the interruption rating to  $I_3$ .

ties that are unusually favorable for quenching the electric arc in a circuit breaker.

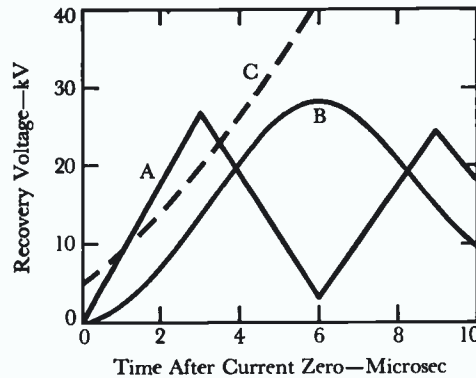
The ability to carry away the power generated by the switching arc is an essential requirement of the gas in a gas-blast circuit breaker. When this ability is inadequate, the arc "clogs" the interrupter nozzle, interfering drastically with the interruption process. The superiority of SF<sub>6</sub> over air is evident in its ability to carry away energy with a lower temperature rise (Fig. 2).<sup>3</sup>

High-power circuit breakers generally meet their most difficult test when interrupting a heavy fault located only a short distance out on a transmission line. The RRRV for this condition is equal to the line surge impedance times the rate of change of fault current just before current zero. The sawtooth line voltage oscillation, superimposed on the more slowly rising bus recovery voltage, reaches crest value in a relatively few microseconds. Thus, the success or failure of interruption is determined in a very short time after current zero. For this reason, the small arc time constant of SF<sub>6</sub> gas permits interruption of much higher values of fault current than does compressed air without special means such as shunt resistance to reduce the RRRV.

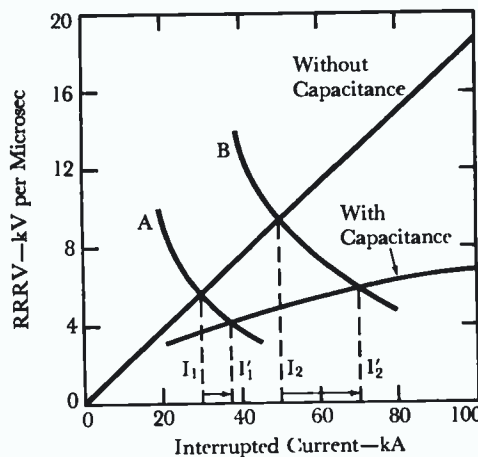
At the higher breaker ratings, with either air or SF<sub>6</sub>, the limiting phenomenon is arc reignition in the presence of residual arc column conductance ("post-arc current") where energy balance is critical. Recent calculations,<sup>3</sup> employing boundary layer techniques and radial diffusion theory, have led to an approximate formula for the critical rate of rise of recovery voltage per break in a gas blast circuit breaker:

$$RRRV = \frac{K P^{1.25} f(l, L)}{(di/dt_0)^n} \quad (1)$$

where  $K$  is a coefficient dependent on gas properties and arc column temperature,  $P$  is absolute gas pressure at nozzle throat,  $di/dt_0$  is rate of approach of arc current to zero,  $l$  is effective arc length (some fraction of total arc length),  $L$  is arc length upstream of the minimum nozzle cross section, and  $n$  is an exponent between 1 and 1.5.



4—After a short line fault, the line-side recovery voltage appears as curve A. At the first intersection of curve C (a typical dielectric recovery) with curve A, the arc reignites. If shunt capacitance is added on the line side of the breaker, the recovery voltage assumes the more slowly rising 1-cosine waveform of curve B. Since curve C now is not intersected, the arc does not restrike.



5—Adding line shunt capacitance improves any breaker, but those with higher inherent capability show greater improvement. Curve B, for example, represents a breaker having higher inherent interrupting ability than the breaker of curve A ( $I_2 > I_1$ ); when shunt capacitance is added to both breakers, breaker B will show the greater improvement. Thus shunt capacitance can be particularly beneficial to breakers using SF<sub>6</sub>, since the arc time constant of the gas is lower than that of air.

Relative values of the coefficient  $K$  for SF<sub>6</sub> and for air depend strongly on the arc column temperatures. Recent theoretical and experimental studies have shown that much higher temperatures are required to sustain arcs in a blast of SF<sub>6</sub> than in similar blasts of compressed air and that the arc column diameter is much smaller in SF<sub>6</sub>. These are important reasons for the improved performance of SF<sub>6</sub> over air.

**SF<sub>6</sub> Interrupter Design and Application**—Results of the fundamental studies reported are being applied to interrupter design. Gas pressure and mass flow with specific orifice configurations are important parameters being considered in avoiding clogging and providing means for dissipating the enthalpy associated with the arc. To interrupt the higher fault currents, it is important that dielectric recovery "win the race" with the line voltage rise in the few microseconds available after current zero. Winning the race depends largely on the successful discharge of heated gas and the envelopment of the arc core with cool high-pressure gas just prior to current zero.

For practical applications, equation 1 can be simplified as follows, assuming a fixed system frequency and a particular orifice configuration, and using the more conservative value of 1.5 for  $n$ :

$$RRRV \text{ (Interrupter)} = K_1 \frac{P^{1.25}}{I^{1.5}} \text{ kV}/\mu\text{sec.} \quad (2)$$

Also, for a surge impedance of 450 ohms, a system frequency of 60 Hz ( $\omega = 377$ ), and  $I$  in kiloamperes, the short line fault recovery rate is:

$$RRRV \text{ (System)} = \sqrt{2}\omega Z I \times 10^{-6} = 0.24 I \text{ kV}/\mu\text{sec.} \quad (3)$$

Fig. 3 illustrates for a short line fault the relationship between the RRRV and current for the system, from equation 3, as curve A and also the capability of an interrupter, from equation 2, as curve B. For low values of current the RRRV applied is low, whereas the typical interrupting capability is high. At the higher values of current the reverse is true. The intersection of the two curves represents the maximum interrupting current for which the breaker can be rated.

By varying the parameters discussed earlier, this capability curve can be shifted to the right as in curve *C*. A significant way of doing so is raising the pressure at the orifice, which is affected by the size and location of the blast valve. When the valve is placed upstream from the contacts, it can be smaller than a valve located downstream, which must discharge a larger volume of heated gas. A favorable valve location right at the contacts has been obtained in at least one arrangement by using the contacts themselves as a blast valve. This provides for maximum pressure difference and gas flow immediately upon contact parting. Dynamic gas flow studies under conditions of arcing indicate that a gradually expanding orifice with an angle of 9 to 15 degrees provides optimum conditions for discharging the heated gas.

#### Series Breaks

Having optimized the factors bearing on the inherent interrupting capability of one break, higher breaker ratings can also be obtained by reducing the RRRV to be handled by a single break. This can be accomplished by using two or more breaks in series, with added capacitance across each break to improve the division of voltage. The effect of using two breaks in series to obtain higher short line fault capability is shown by curve *D* in Fig. 3. The improvement, although appreciable, is not a linear function of the increased number of breaks but calculates for an assumed 55-percent/45-percent voltage distribution to be:

$$I_3/I_2 = (1/0.55)^{0.4} = 1.27.$$

#### Line-Side Shunt Capacitance

The line-side recovery voltage transient following a short line fault interruption beyond the first peak oscillates about the more slowly rising bus-side voltage as illustrated by curve *A* in Fig. 4. When several thousand picofarads of shunt capacitance is added on the line side of the breaker,<sup>4</sup> the voltage transient has a somewhat lower frequency, but more importantly takes the shape of the wave function 1-cosine, as shown by curve *B*. The near-zero initial slope of this type of recovery voltage is especially helpful to an

SF<sub>6</sub> interrupter, in which the arc time constant of the gas is extremely low.

Curve *C* of Fig. 4 is a typical dielectric recovery. It starts at a value generally between one and two times the arc voltage just prior to current zero. At the intersection of the unmodified sawtooth transient and the dielectric recovery curve, the arc is presumed to reignite. However, the more slowly rising recovery voltage transient, as a result of added line-side capacitance, would not cause a restriking in a breaker having the indicated dielectric recovery characteristic.

A breaker having an inherent high current interrupting ability, i.e., with a short arc time constant, shows a larger percent improvement in performance by the addition of a given amount of capacitance than a breaker of lower inherent ability. This explains why a highly effective SF<sub>6</sub> breaker benefits from relatively small amounts of added line capacitance, whereas a compressed-air breaker without resistors would require prohibitive amounts of capacitance to achieve a comparable interrupting ability.

A specific example of uprating by the use of shunt capacitance is shown in Fig. 5. By connecting several thousand picofarads of shunt capacitance on the line side of a breaker that is normally capable of interrupting 30 kA on a short line fault, the rating can be raised 23 percent to a value of 37 kA. However, if the inherent capability of a more effective breaker is as high as 50 kA, then the same added capacitance will increase the rating as much as 40 percent to 70 kA. It is important that blast valve sizes and vent areas are also enlarged, if required, to assure that the interrupter nozzle will not clog as the current rating is raised.

#### Summary

Controlling the switching surges encountered in prospective EHV and UHV power systems requires new concepts of circuit breaker design and operation. The superiority of SF<sub>6</sub> gas over compressed air for arc interruption and quenching makes it a particularly favorable gas for use in such breakers. Its use in modular breaker designs provides any one of three different levels of closing

switching surge limitation. A single step of resistor insertion maintains transients within 2.0 per unit. Two resistance steps can be included if a limit of 1.7 per unit must be met. If in addition to two-step resistors, the closing of the main contacts is controlled in each phase with respect to the voltage across the resistance, the closing transients can be kept below 1.5 per unit.

Studies of gas properties, interrupter nozzle design, and blast valve location have also led to improvements in breaker performance when interrupting high-current short circuits. Formulas have been derived to show the dependence of the rate of rise of recovery voltage that can be withstood on the gas pressure at the nozzle and on the current to be interrupted.

For circuit breakers that use SF<sub>6</sub>, with its characteristically small arc time constant, a very substantial increase in current interrupting rating under short line fault conditions can be obtained by the addition of several thousand picofarads of shunt capacitance on the line side terminal.

#### REFERENCES:

- <sup>1</sup>R. N. Yeckley and C. F. Cromer, "New SF<sub>6</sub> EHV Breakers for 500 kV and 765 kV," IEEE Winter Power Meeting, January 25-30, 1970, Paper No. 70 TP 111-PWR.
- <sup>2</sup>R. G. Colclaser, Jr., C. L. Wagner and E. P. Donohue, "Multi-Step Resistor Control of Switching Surges," IEEE Trans. PA&S Vol. 88, July 1969.
- <sup>3</sup>B. W. Swanson, R. M. Roidt, T. E. Browne, Jr., "The Effect of Gas Dynamics and Properties of SF<sub>6</sub> and Air on Short Line Fault Interruption," IEEE Winter Power Meeting, January 25-30, 1970, Paper No. 70 TP 113-PWR.
- <sup>4</sup>R. G. Colclaser, Jr., L. E. Berkebile and D. E. Buettner, "The Effect of Capacitors on the Short Line Fault Component of Transient Recovery Voltage," IEEE Winter Power Meeting, January 25-30, 1970, Paper No. 70 TP 176-PWR.

# Nonconsumable Electrode Makes Vacuum Arc Melting More Economical

Ronald R. Akers

*The Durarc nonconsumable electrode reduces the cost and complexity of vacuum arc melting by eliminating the conventional electrode fabrication step and by providing for efficient utilization of scrap. Water cooling and high-speed rotation of the arc permit high-power melts at low tip erosion rates.*

Many components used in today's advancing technologies, especially in the aerospace field, demand specialized construction materials. They must be strong, lightweight, corrosion resistant, and able to withstand high temperatures. A material with such properties is titanium. Although titanium is the ninth most abundant element in the earth's crust, it has remained, until recently, in the class of rare metals mainly because of its great affinity for carbon, nitrogen, and oxygen and the resulting difficulty of processing it under controlled conditions.

One step in titanium metal production is the reduction of titanium tetrachloride with magnesium or sodium to form titanium sponge, a porous material containing mostly chloride impurities. The sponge is then purified and consolidated by electric arc melting in an inert atmosphere or, preferably, under vacuum where impurities are vaporized and drawn off as gases.

Consumable-electrode arc melting has been the most widely used technique. A consumable electrode is formed by compressing sponge into briquets, which are then welded together. The electrode is then melted in the furnace by passing a high current through it to draw an arc between the tip and a bit of pure metal (striker) in the bottom of the water-cooled copper ingot mold. While the electrode is being consumed into a molten pool, a vacuum pump draws out the gaseous impurities. To reduce the amount of impurities and to improve homogeneity still further, an ingot formed in this way is often used as the consumable electrode for a second melt cycle.

As well developed as consumable-electrode melting is, it still has a number of limitations:

1) The cost of fabricating the initial electrode from sponge is a sizeable portion of the melting cycle costs.

2) Scrap is difficult to reclaim efficiently because of the necessity to fabricate it into an electrode, and there is danger that tool bits (tungsten carbide etc.) and other high-density materials present in the scrap may not get melted and carry through the process into the final ingot.

3) Flow of gaseous impurities from the melt is restricted by small clearances between the molten pool, the electrode, and the mold walls.

4) Melt rate is directly proportional to power level, allowing little independent control of melt temperature.

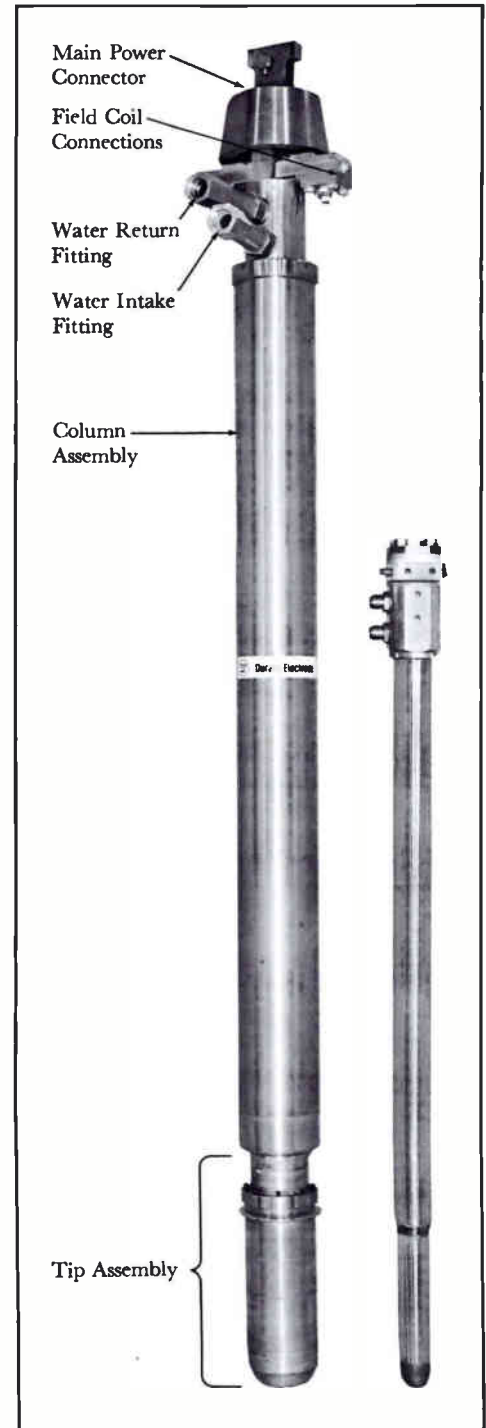
To overcome these difficulties, the Westinghouse Power Circuit Breaker Division has developed a melting technique employing the new Durarc nonconsumable electrode for the first melt. The resulting ingot is then used as the electrode for a consumable-electrode second melt.

## **The Durarc Electrode**

The electrode consists of four basic sections: tip, tip assembly, column assembly, and header assembly (Fig. 1). The copper tip is hollow and has threaded inner walls for easy removal from the assembly. Encapsulated within the tip is one of the unique features of the Durarc electrode, a cylindrical field coil that generates a magnetic field having a large flux component parallel to the tip surface (Fig. 2). When an arc is drawn between the tip and the melt, its interaction with the magnetic field forces the arc to rotate over the tip surface; this distributes the intense heat of the arc uniformly and prevents local damage to the tip.

The tip is efficiently cooled by high pressure water circulating between the cup containing the field coil and the tip itself (Fig. 3). The tip assembly, like the tip, is easily removed for rapid change or inspection.

The column assembly has a stainless steel outer surface, which forms a move-



1—On the left, the main features of the four assemblies of a 4-inch diameter Durarc electrode are shown. The other is a newly developed 2-inch electrode used for experimentation in small furnaces at the Westinghouse Research and Development Center.

Ronald R. Akers is an Arc Heater Engineer at the Power Circuit Breaker Division, Westinghouse Electric Corporation, East Pittsburgh, Pennsylvania.

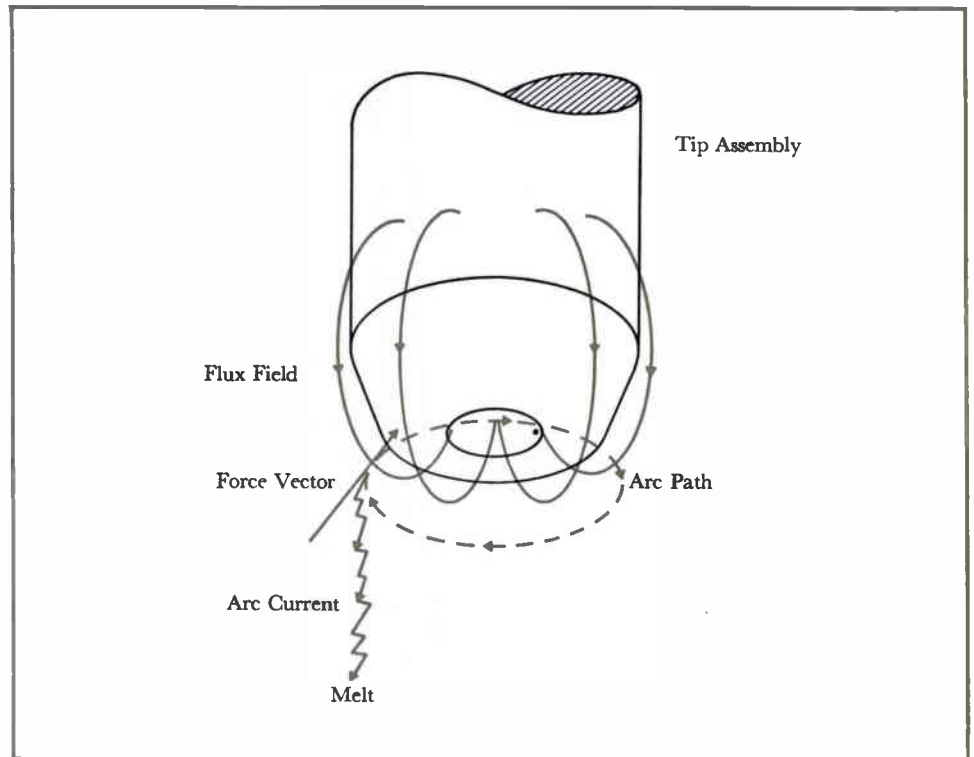
able seal with the furnace to permit vertical maneuvering during melting operations. Arc power is transferred from the power connection in the header assembly to the tip assembly through an inner copper sleeve to provide good electrical connection and minimize power losses. These concentric columns also provide the water passage to the tip. Connections for mechanical support, water lines, and field coil power are also located in the header assembly. As the center of the entire electrode is open, gases such as helium or argon can be injected into the furnace if an inert atmosphere is desired.

Basic requirements for electrode operation, in addition to normal arc furnace equipment, include a cooling water system and a low-voltage, high-current dc power supply to energize the magnetic field coil. The water pump is generally of the 100-gal/min class with a 35- to 75-horsepower motor. In addition, there are valves for water flow control and interlocks to prevent the electrode from operating without a magnetic field and proper water circulation. Temperature and flow monitoring devices are also included.

### *Nonconsumable-Electrode Melting*

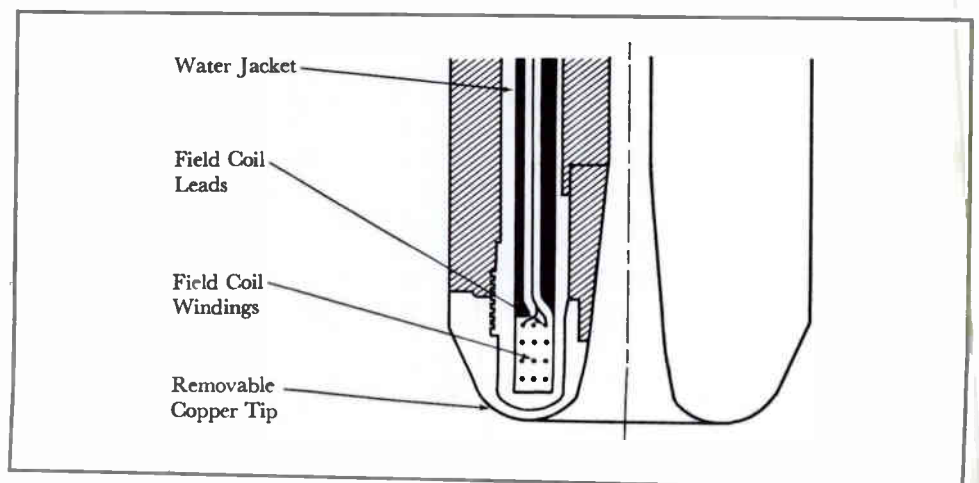
Once an arc has been struck between the electrode and striker, and a molten pool formed, the material to be melted is fed into the furnace from a hopper by a suitable feeding system. Material is continuously melted until the desired size ingot is built up. As the ingot grows, the electrode is gradually withdrawn to maintain an adequate arcing distance.

Durarc electrodes of 2, 4, 8, and 16 inches in diameter have been tested in various melting applications. Titanium and zirconium sponge, Inconel, molybdenum, Monel, Stellite, chromium, and various stainless steels have been successfully melted with 2- and 4-inch electrodes. Ingot mold sizes vary somewhat in proportion to electrode diameter. For instance, considerable research has been performed with a 2-inch-diameter electrode (similar to the 2-inch electrode in Fig. 1) and a 4-inch mold, whereas 4-inch electrode and a 25-inch mold.



2—Illustrated schematically is how arc rotation is accomplished when the Durarc electrode is in operation. When an arc is struck between the tip and melt, the direction of the arc current is toward the melt. Since the flux field is parallel to the tip surface, it is perpendicular to the arc current.

Their interaction produces a force vector perpendicular to them both such that the arc rotates around the electrode tip in the indicated direction. This action distributes the heat uniformly over the tip surface and thereby prevents local tip damage.



3—This cutaway view of a Durarc electrode's tip assembly indicates the relative placement of the internal field coil and the water pas-

sages within the tip and tip assembly. Also visible are the tip's inner threaded walls for easy removal from the assembly.

Most melt operations have been performed in the pressure range from 2 to 200 torr, although Durarc electrodes have been tested from  $2 \times 10^{-3}$  torr to atmospheric pressure.

Power levels for most of the testing in research furnaces have been in the 300- to 450-kW range at the maximum available current level of 8500 to 10,500 amperes, depending on arc voltage. These power levels give suitable results for titanium sponge at feed rates to at least 12 pounds per minute in 15- and 19-inch molds, and material has been melted at rates as high as 15 pounds per minute. In larger scale operations, a power level of 750 kW at 19,000 amperes has been successfully used in melting stainless steel, and titanium ingots of 4000 pounds have been melted from sponge at 15,000-ampere arc currents.

Various melting experiments have proven that tip life can be significantly extended if the electrode is made positive and the mold made negative, instead of the opposite polarity arrangement used in consumable-electrode melting. Tip life also depends much on the type of material being melted. A tip used for melting titanium sponge, which has considerable chloride impurities, might have an expected operating life of 40 to 100 hours, while one used in melting stainless steel, having fewer impurities, has a projected life of more than 250 hours. In general, copper contamination of the melt from the electrode tip is not a problem because of the tip's slow erosion rate. A typical erosion rate is about  $1\frac{1}{2}$  grams per hour, which, with a feed rate of 10 pounds per minute, would give a contamination level of less than 6 parts per million.

### Advantages

**Operational**—A melting procedure utilizing the Durarc nonconsumable electrode exclusively, or in conjunction with consumable-electrode remelting, overcomes the four limitations of exclusive consumable-electrode melting:

1) The electrode fabrication step is not needed, since the ingot formed by nonconsumable melting becomes an electrode for a consumable-electrode melt cycle.

2) Any desired ratio of scrap to sponge can be successfully melted with the Durarc electrode, and scrap size is limited only by mold dimensions. Processes are also being developed to study the removal of high-density inclusions from contaminated scrap.

3) The area above the molten pool is virtually open for removal of impurity gases because of the longer arc gap. Better gas passage also results from larger electrode-to-mold clearances.

4) Power level can be controlled independently of melt rate. This allows the user more flexibility; for instance, by keeping the pool at a higher temperature, high-melting-point alloys go into solution more easily. Moreover, when castings are to be poured, the molten pool can be superheated by continuing to arc after the feed material has been completely consumed. This makes the material more fluid and allows pouring of more intricate and complicated castings.

Independent power control also allows "hot topping" of ingots. At the end of a consumable ingot melt, a large molten pool remains that shrinks as it solidifies, resulting in internal gaps or shrinkage cavities. As much as 30 percent of the ingot may contain cavities. However, by placing a Durarc electrode over the ingot and keeping the upper surface molten, the shrinkage area can be "fed," resulting in a smooth and homogeneous ingot.

**Economic** — Nonconsumable-electrode melting of sponge probably is most attractive for a new melt shop or for one in which added capacity is desired but would require purchasing new electrode fabrication equipment. Eliminating the need for fabricating electrodes from sponge saves not only the cost of a compacting press but also the cost of installation, foundations, auxiliary equipment, perhaps a building, and the required manpower. Welding and handling equipment for electrode fabrication would also be saved.

The cost of alloy preparation equipment is the same as that for the electrode fabrication process. Furnace cost is increased by the feeding mechanism, cooling system, field coil power supply, and the associated control systems. Cost of

the Durarc electrode—replacement parts, tips, and rental charges—varies with the operating practices and production volume of the individual plant.

To summarize, a substantial saving arises from the lower original equipment investment plus saving of the labor otherwise required for electrode fabrication. The main savings, however, will result from recycling scrap into ingots or castings. Presently, the titanium industry generates nearly as much scrap in a year as is shipped in the form of mill products. A major portion of this is currently not recycled, primarily because of the danger of high-density inclusions. The Durarc electrode, however, offers an excellent tool for the recovery of this scrap and can provide a substantial savings to the industry: original titanium sponge is worth over one dollar per pound, whereas the scrap is often sold at 2 to 20 cents per pound.

Other significant cost reductions and process improvements will result from the electrode's independent control of melt temperature for both superheating and hot topping.

### Application and Development

Initial vacuum testing of the Durarc electrode was conducted at the Westinghouse Research Laboratories. Since then, larger scale testing has been performed with the Crucible Specialty Metals Division of Colt Industries, Midland, Pennsylvania. A Durarc electrode is presently in use melting titanium at Titanium Technology Corporation (owned by Carpenter Technology Corporation), Pomona, California. The Westinghouse Specialty Metals Division, Blairsville, Pennsylvania, uses an electrode in studies concerning the melting of zirconium, titanium, Kovar, Inconel, and various superalloys.

Design and application research continues. The new 2-inch electrode shown in Fig. 1, for example, has recently been developed for use in small casting furnaces and for research and development investigations. Studies continue for the development of processes to improve scrap recovery and to prove the benefits of superheating and hot topping.

# Technology in Progress

## Pittsburgh Stadium Gets Long-Life Maintenance-Free Floodlights

Floodlighting equipment in Pittsburgh's new Three Rivers Stadium should need little or no maintenance for as long as 15 years, because the long-life mercury floodlights used have pressure-sealed airtight optical systems that exclude air, dirt, and moisture. (See photograph on outside back cover.)

Standard floodlights "breathe," or take in air, so dirt accumulating inside on the reflector and lens reduces lamp efficiency as much as 30 percent; for that reason, they must be opened and cleaned at least once a year. The new floodlight, however, is "non-breathing" and so doesn't have to be cleaned.

The Three Rivers Stadium has 1632 of the MLS (for "major league stadium") floodlights. Each has a 1000-watt metal-halide mercury lamp with a rated life of 7500 hours. The lights will be used an estimated 500 hours a year and therefore should not require service for about 15 years. Aside from lamp aging, the only drop-off in light output will come from dirt accumulation on the exterior of the floodlight lens, which lighting studies show cuts lamp efficiency by a negligible three percent.

Pittsburgh's stadium will be one of the brightest ballparks in the world. The high-efficiency lamps will produce nearly 100 lumens per watt, more than twice the output of a standard mercury lamp and five times that of an incandescent lamp. The baseball infield will be bathed in 400 footcandles of light; the outfield, 250 footcandles; and the football field, 300.

The floodlight lamp is installed at the plant and the optical system sealed. To mount the unit, workmen connect the incoming cable to terminals in a wiring compartment. The floodlight can be aimed with precision.

Although similar in principle to an automobile sealed-beam headlamp, the MLS fixture is not thrown away when the lamp burns out, for its door can be re-clamped and resealed after lamp replacement. Development of a method of vulcanizing glass to aluminum made the pressure seal possible.

The MLS light is made by the Westinghouse Outdoor Lighting Department. Although developed for stadium use, it is also suitable for other outdoor applications where high candlepower and maintenance-free service are required.

## Products for Industry

**Load survey recorder**, the WR-1C Pulse-O-Matic, is a two-track magnetic-tape pulse receiver for gathering accurate power data in a form that facilitates computer analysis. A latching relay permits use of either a mechanical or electronic pulse initiator. The tape can be advanced manually without affecting interval or clock time, and interval time and clock can be set independently of tape movement. *Westinghouse Meter Division, P.O. Box 9533, Raleigh, North Carolina 27603.*

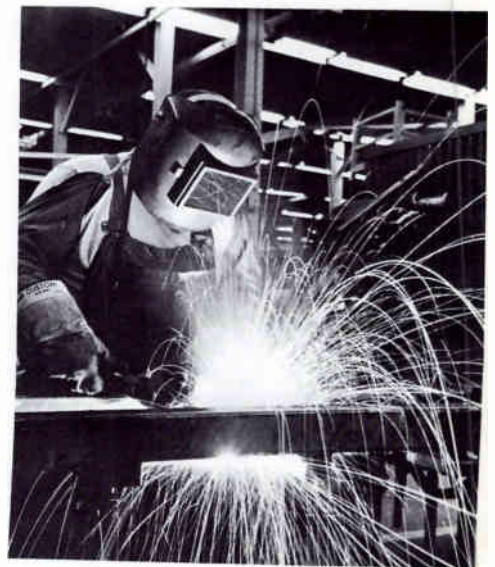
**Heavy-duty centrifugal fans** are standardized units for economical use in incinerators, high-pressure cooling systems, industrial furnaces, and boilers. The 4000S series includes nine fan sizes with diameters from 27 to 60 inches and with discharges pointing in any of five directions. Airfoil blading and the contoured inlet and scroll design give efficiencies as high as 90 percent. The fans provide air volumes from 10,000 to more than 350,000 ft<sup>3</sup>/min with pressures as high as 40 inches of water, at temperatures ranging from -20 to 150 degrees F. *Westinghouse Sturtevant Division, Damon Street, Boston, Massachusetts 02136.*

**Variable-speed ac motor** for pump and fan applications is designed to operate with any type of full-wave thyristor (SCR) voltage controller in applications such as constant-pressure water systems; chemical processes where it is necessary to maintain constant pressures, viscosities, temperatures, or densities; and general water and sewage control systems. The four-pole Adaptiflow motor has a 3-to-1 speed range with a non-reversing speed/torque curve. Its top speed is 1680 r/min, and its design maximizes cooling at any speed. If an abnormal condition does cause over-

heating, Thermoguard protectors on each phase disconnect it from the line. *Westinghouse Medium AC Motor and Gearing Division, 4454 Genesee Street, P.O. Box 225, Buffalo, New York 14240.*

**High-voltage thyristor** provides 2000-volt peak forward blocking voltage without trading off other important characteristics. The type 282-Y40 thyristor carries 400 amperes of half-wave average current and has high surge current capability (up to 7000 amperes), guaranteed dv/dt of 300 volts per microsecond, and low gate current requirement. *Westinghouse Semiconductor Division, Youngwood, Pennsylvania 15697.*

**Arc welding systems** with dual power channels enable operators to switch between two precisely determined volt and ampere settings, with a switch on the torch handle, to weld various gauges of metal without leaving their work. The instant choice of settings can cut equipment needs, improve weld quality, and increase production. SA-505C semiautomatic argon-shielded systems have three basic components—variable-slope power supply with dual power outlets, sealed welding control with remote switch, and gooseneck water-cooled torch. *Westinghouse Welding Department, P.O. Box 300, Sykesville, Maryland 21784.*



*Arc Welding System*

## About the Authors

**William S. Alberts** graduated with a BEE degree from Ohio State University in 1938. He spent 21 years with Crosley Broadcasting Corporation as transmitter operator, research and development engineer, Chief Propagation Engineer, and Director, General Engineering Department. Among his achievements were the engineering design and installation of the radiation systems at the Mason and Bethany plants of the Voice of America.

In 1956, Alberts joined Developmental Engineering Corporation (later known as DECO Electronics, Inc.). He has served as Associate Project Engineer in the design of the radiation system for the Navy's two-megawatt VLF station at Cutler, Maine, as DECO's Project Manager for the design of another two-megawatt Navy VLF communication facility at North West Cape, Australia, and as Project Manager for the Corporation's first contract to develop improved tactical-communications antenna systems for the U. S. fleets. In 1962, he was elected Vice President and Associate Director of the Leesburg Division of DECO. He has participated in the siting and design aspects of valley-span VLF systems and in the siting and consulting activities for the NATO VLF station in Norway. Since the acquisition of DECO by Westinghouse in 1966, Alberts has been Assistant Manager, Operations Manager, Manager of Communications Facilities Engineering, and Consulting Engineer on the modernization of the Navy's earlier VLF facilities and the design of the interim and operational radiation systems and facilities for the Omega navigation system.

**Andrew W. Smith, Jr.**, graduated from North Carolina State College in 1948 with a BSEE degree and came to Westinghouse on the graduate student training program. He joined the metal-working section of the former Industry Engineering group to do control and main-drive application work on large rolling mills. While there, he helped develop the first Prodac card-programmed mill control, and later he developed mathematical models and calculating procedures for on-line control computers for slabbing, hot-strip, plate, and tandem cold mills. Smith moved to the Computer and Instrumentation Division in 1965, where he is presently Rolling Mill Consultant in Metals and Process Systems. His main field of interest now is on-line adaptive computer control of various industrial processes.

**O. J. Aanstad** graduated from the Technical University of Norway in 1963 with the degree of *Sivilingenior* in mechanical engineering. His major subjects were fluid dynamics, prime mover design, and control engineering. He was employed by A/S Kvaerner Brug, Oslo, to work on development of electrohydraulic control systems for hydroturbines, analog

simulations, stability studies, and system analysis. Aanstad joined the Westinghouse Large Turbine Division in 1967 and is now in its controls development group. His responsibilities have included mathematical modeling of large steam turbines, digital simulation, overspeed calculation, and development and specification of turbine controls.

**H. E. Lokay** earned his BSEE degree in 1951 from Illinois Institute of Technology and his MSEE degree from the University of Pittsburgh in 1956. He joined Westinghouse in 1951 on the graduate student training program and later became part of the distribution engineering group of the Electric Utility Engineering Department. In 1959 he was made a Sponsor Engineer, working with utilities and consulting engineering firms on equipment application and systems engineering. In 1967 Lokay was named Manager, Rotating Machinery, Power Systems Planning. His group's activities include working with Westinghouse divisions and with electric utilities on engineering and associated problems in power generation and generation planning. He was coeditor of Volume III of the *Westinghouse Electric Utility Engineering Reference Book*.

**W. M. Leeds** graduated from Haverford College in 1926 with a BSEE and, in 1930, earned his MSEE from the University of Pittsburgh. He attended Massachusetts Institute of Technology in 1937 and later received a PhD degree in Physics-Engineering at the University of Pittsburgh. Dr. Leeds joined Westinghouse in 1926 as a power circuit breaker engineer, and in 1938 he was made Manager of the PCB Development Section. He has since been Manager of Long Range Major Development in the Switchgear Division and in the PCB Division.

Dr. Leeds became Manager of the PCB Engineering Department in 1961 and Manager of the New Product Department in 1963. In 1968, he assumed his current position as PCB Consulting Engineer. Dr. Leeds has made significant contributions to circuit breaker technology, including development of "De-ion" grid interrupters, use of SF<sub>6</sub> gas, and design of EHV breakers. He has accumulated 90 patents.

**R. E. Friedrich** graduated from the University of Pittsburgh, where he received a BS in Physics in 1940 and an MS in 1953. He joined Westinghouse on the graduate student training program in 1940 and joined the Power Circuit Breaker Division to work in breaker design. In 1955 Friedrich was made Manager, Development Section. His other management positions at the PCB Division have been in the Large SF<sub>6</sub> Breaker Development Section and the EHV Circuit Breaker

Section. He is presently Manager, New Products Development Section. Friedrich has helped develop De-ion grid interrupters for oil breakers, "dead-tank" breakers using SF<sub>6</sub> gas, and a new line of porcelain-column, modular, EHV SF<sub>6</sub> breakers.

**Charles L. Wagner** received a BSEE from Bucknell University in 1945 and earned his MSEE from the University of Pittsburgh in 1949. He joined Westinghouse in 1946, working at the Engineering Laboratories where he helped develop the Anacom analog computer. In 1950 he became a Sponsor Engineer for the Southeastern region of the United States and, in 1954, a Sponsor Engineer for the Atlantic region, where his work consisted of assisting electric-utility and industrial customers in problems of equipment application, system planning, and design. Wagner became Project Manager of the VEPCO 500-kV project in 1962 and also Engineer-in-Charge of the Relaying and Metering Groups for the other Westinghouse EHV study projects. He is now Manager, Transmission Control and Protection, Power Systems Planning.

**T. E. Browne, Jr.**, received a BSEE from North Carolina State University in 1928, an MSEE from the University of Pittsburgh in 1933, and his PhD degree in 1936 from California Institute of Technology where he also served as a graduate assistant. Dr. Browne joined Westinghouse in 1928 and worked first at the Research Laboratories on arc phenomena and circuit interrupting devices. In 1951, he became a Fellow Engineer in switchgear engineering. He later was named Supervising Engineer and then Section Manager for Long Range Major Development of Interrupting Devices. He is currently Section Manager, Long Range Major Development Laboratory. Dr. Browne has been responsible for or contributed to the development of oil, air-blast, and SF<sub>6</sub> circuit breakers and high-voltage insulation.

**Ronald R. Akers** joined Westinghouse on the graduate student training program in 1961 when he received a BSME degree from Iowa State University. He spent his first year at the Westinghouse Research Laboratories on the Advanced Mechanics Program, earning an MSME degree at the University of Pittsburgh. In 1962, Akers transferred to the Astronuclear Laboratory and began development of an MHD space power plant. Two years later, he became project engineer on advanced arc heaters for simulation of spacecraft reentry conditions at the Power Circuit Breaker Division. In 1966, Akers assumed his present position as Project Engineer, responsible for the development, design, application, and marketing of Durarc nonconsumable electrodes for vacuum metals melting.

Westinghouse ENGINEER  
Westinghouse Electric Corporation  
Westinghouse Building  
Gateway Center  
Pittsburgh, Pennsylvania 15222

Address Correction Requested  
Return Postage Guaranteed

The Library  
University of Vermont  
Burlington, Vermont 05401

CML-18

Bulk Rate  
U. S. Postage  
**PAID**  
Lancaster, Pa.  
Permit 1582



Maintenance-free floodlights for new Pittsburgh stadium. (Information on page 128.)